ENGINEERING RESEARCH INSTITUTE
UNIVERSITY OF MICHIGAN
ANN ARBOR

CALCULATION OF A WAVE-GUIDE-LOADED RESONATOR FOR INTERDIGITAL MAGNETRONS

Technical Report No. 14
Electron Tube Laboratory
Department of Electrical Engineering

By

GUNNAR HOK

Approved by: W. G. DOW

September, 1952

TABLE OF CONTENTS

ABSTRACT

Part I. General Analysis of Discontinuities in Wave Guides and Cavities.

The transmission and reflection of electro-magnetic waves at the boundary surface between two systems of different geometry is studied by means of harmonic analysis. Attention is at first focused on such configurations that two-dimensional rather than three-dimensional analysis is possible. An equivalent network is given and a comprehensive expression derived for the wave admittance of the discontinuity in terms of the wave admittances of the normal anodes in the two systems and the coefficients of coupling between them. A coefficient of coupling is defined as a normalized non-orthogonality integral of the wave functions over the boundary surface between the two systems. The result is directly applicable to wave-guide junctions and is extended to symmetrical obstacles in wave guides by combination of symmetrical and antisymmetrical illumination of the two discontinuities. Equivalent open-circuit and short-circuit impedances, T and π networks are given. The more general problem of three-dimensional harnomic analysis is considered in connection with a specific example: the junction between a rectangular wave guide and a cylindrical resonator. The general solution as well as an explicit approximate formula for the admittance of the junction are derived.

Part II. Solution of the Specific Problem.

This part of the paper considers the problem of designing a wave-guide-output system for an interdigital magnetron so as to realize a specified slot conductance for the electronic operation of the magnetron. First the electromagnetic field at resonance is calculated in all parts of the system. Then the impedance transformation between the anode and the output wave guide is designed to meet the specifications. To facilitate experimental verification of the results, expressions are derived for the external and the internal Q of the resonator. Test results on a scale model are given and compared with computed values.

LIST OF ILLUSTRATIONS

PART I

PART II

CALCULATION OF A WAVE-GUIDE-LOADED RESONATOR FOR INTERDIGITAL MAGNETRONS

PART I GENERAL ANALYSIS OF DISCONTINUITIES IN WAVE GUIDES AND CAVITIES

INTRODUCTION

The application of harmonic analysis to electromagnetic fields in wave guides and cavities, as well as to junctions between or discontinuities within such systems, is well established.[1-10] It is also well known that the usefulness of harmonic analysis for numerical calculation is somewhat restricted by the slow convergence of the series obtained in many problems. Nontheless it is felt that the formulas and equivalent networks developed in this paper may be of appreciable interest.

The electromagnetic waves propagated in wave guides, along wires, or radiated from antennas are conventionally expressed as a sum of a number of components which have the form of the normal modes of the system. Each normal mode is one of the orthogonal solutions of the vector wave equation consistent with the boundary conditions; the wave equation being referred to such a coordinate system x_1, x_2, x_3, that each boundary surface characteristic of the geometry satisfies one equation x_μ = constant. These boundaries are assumed to have infinite conductivity. The normal modes of a system form a complete set of orthogonal functions, so that any field configuration that is solenoidal and satisfies Maxwell's equations and the boundary conditions can be expressed as a Fourier series in terms of the orthogonal modes.

When two such systems of different geometry are joined together, so that waves travel from one system into the other, it is theoretically possible to solve any wave propagation problem in terms of the normal modes of one system alone by application of the appropriate boundary conditions. After the field configuration in the second system is obtained in this way it can be translated in terms of the normal modes of the second system by harmonic analysis. A considerable simplification of the computations results if the translation can take place right at the boundary surface where the waves leave one system and enter the other, that is, if the harmonic analysis can be performed in two dimensions rather than in three. This is possible if the common boundary between the two systems is contained in a surface x_μ = const. in both coordinate systems. We shall begin by considering problems of this character.

A. TWO-DIMENSIONAL HARMONIC ANALYSIS

Fig. 1 is a schematic representation of a junction of two wave guides or cavities. The natural modes of the system to the left of the boundary are most simply described in terms of the orthogonal coordinates x_1, x_2, x_3; those of the system to the right in terms of y_1, y_2, y_3. The common boundary S is included in a surface $x_3 = 0$ which is also $y_3 = 0$. The cross section of the left wave guide, as measured along this coordinate surface, is A, the cross section of the right one B. The tangential electric field in S can be expanded in terms of the natural modes of both wave guides. Since the tangential electric field is zero over those parts of A and B not belonging to S, each expansion is uniquely determined by the field configuration over S.

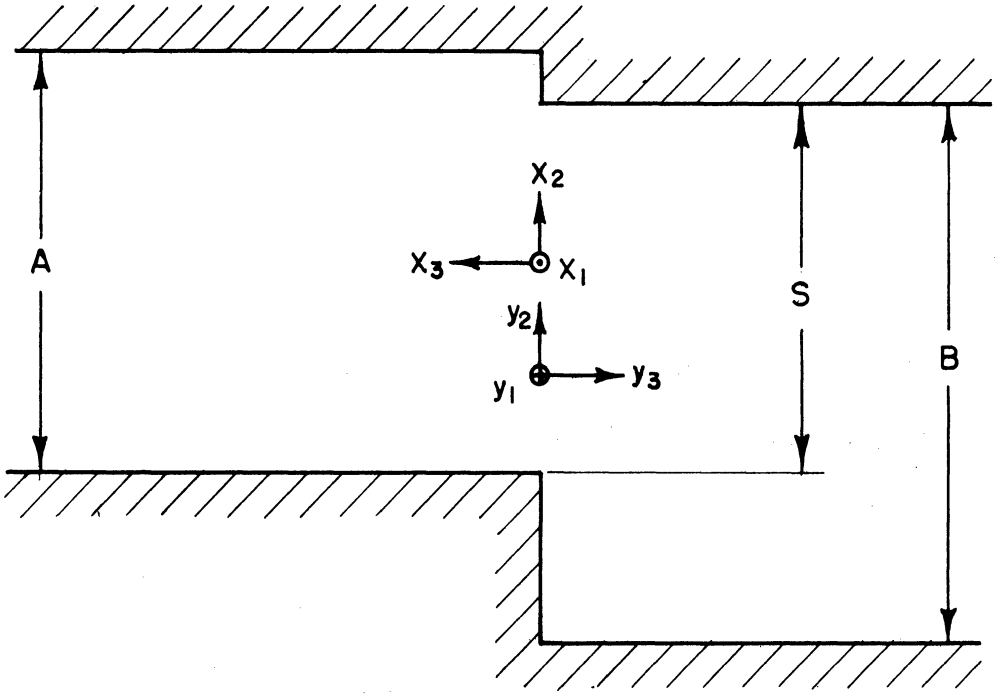

FIG. 1
SCHEMATIC REPRESENTATION OF THE JUNCTION OF TWO DIFFERENT WAVE GUIDES

$$E_s\,(x_1,x_2) = E_{A1}\,e_{A1}\,(x_1,x_2) + E_{A2}\,e_{A2}\,(x_1,x_2) + \ldots \quad (1)$$

$$E_s\,(y_1,y_2) = E_{B1}\,e_{B1}\,(y_1,y_2) + E_{B2}\,e_{B2}\,(y_1,y_2) + \ldots \quad (2)$$

Here the two-dimensional orthogonal functions e_{Av} and e_{Bv} are normalized to unity so that

$$\int_A e^2_{A_v}\,dx_1\,dx_2 = 1\ , \quad (3)$$

$$\int_B e^2_{B_v}\,dy_1\,dy_2 = 1\ . \quad (4)$$

We shall in this section limit the scope of the analysis to systems that are symmetrical and permit us to choose the coordinates so that $y_1 = -x_1$ and $y_2 = x_2$ on the boundary surface.

Equating the right members of (1) and (2), multiplying by one orthogonal function at a time and integrating, we obtain the following relations between the coefficients in the two expansions

$$\left.\begin{aligned} E_{B1} &= \alpha_{11}E_{A1} + \alpha_{21}E_{A2} + \ldots\ldots\ldots\ldots \\ E_{B2} &= \alpha_{12}E_{A1} + \alpha_{22}E_{A2} + \ldots\ldots\ldots\ldots \\ &\ldots\ldots\ldots\ldots\ldots\ldots\ldots\ldots \end{aligned}\right\}\ , \quad (5)$$

$$\left.\begin{aligned} E_{A1} &= \alpha_{11}E_{B1} + \alpha_{12}E_{B2} + \ldots\ldots\ldots\ldots \\ E_{A2} &= \alpha_{21}E_{B1} + \alpha_{22}E_{B2} + \ldots\ldots\ldots\ldots \\ &\ldots\ldots\ldots\ldots\ldots\ldots\ldots\ldots \end{aligned}\right\}\ , \quad (6)$$

where the coefficients of coupling α are defined by the nonorthogonality integrals:

$$\alpha_{\mu\nu} = \int_S e_{A\mu}\, e_{B\nu}\, dx_1\, dx_2 \quad . \tag{7}$$

The tangential magnetic field components in S associated with each normal mode in the two guides are related to the tangential electric field components by the wave admittances according to the equations

$$H_{A\nu} = E_{A\nu}\, \bar{Y}_{A\nu} \tag{8}$$

$$H_{B\nu} = E_{B\nu}\, \bar{Y}_{B\nu} \tag{9}$$

With the coordinate systems chosen, all wave admittances are positive for waves propagated away from the junction and negative for waves traveling towards the junction.

The continuity of the tangential magnetic field over the area S requires that the sum of all the B-components equals the sum of all the A-components. Since the tangential magnetic field is not zero over the areas of A and B not included in S, this condition allows many different expansions of the magnetic field in terms of the normal modes of guides A and B. The correct expansions have to be compatible with the expansions of the transverse electric field and the wave admittances of the individual modes as well as with the continuity relations over S.

$$-H_s = E_{A1}\, \bar{Y}_{A1}\, e_{A1} + E_{A2}\, \bar{Y}_{A2}\, e_{A2} + \cdots\cdots\cdots \tag{10}$$

$$+H_s = E_{B1}\, \bar{Y}_{B1}\, e_{B1} + E_{B2}\, \bar{Y}_{B2}\, e_{B2} + \cdots\cdots\cdots \tag{11}$$

Since H_A and H_B are not zero outside S the procedure leading from (1) and (2) to (5) and (6) can not be duplicated for the magnetic field. This difficulty can be overcome by introduction of a third set of orthogonal functions over S and use of this set as an intermediate step between the sets $e_{A\nu}$ and $e_{B\nu}$. We shall do this later on but first solve the problem for a simple case where this is not necessary.

Special Case: S = A

When all the area A is included in the common boundary S, we can apply to H_s all orthogonality relations that involve integration over A only. Then multiplying the right members of (10) and (11) in turn by each one of the functions $e_{A\nu}$ and integrating over A we get

$$\left.\begin{aligned} -H_{A1} &= \alpha_{11} H_{B1} + \alpha_{12} H_{B2} + \cdots\cdots\cdots \\ -H_{A2} &= \alpha_{21} H_{B1} + \alpha_{22} H_{B2} + \cdots\cdots\cdots \\ &\cdots\cdots\cdots\cdots\cdots\cdots\cdots\cdots \end{aligned}\right\} \quad . \quad (12)$$

It is important to note that in this system of equations we must always include a considerably larger number of terms that the number of equations, since the H_B-components determine the H_A-components buy not vice versa.

Between (5), (8), (9), and (12) it is now possible to eliminate all field components but one set, for instance $E_{A\nu}$. The result is a complete system of homogeneous linear equations between those components. Its solution is either $E_{A\nu} = 0$, or the determinant of the coefficients must varish. The former is the case if all the admittances are passive (no waves approaching the junction); on the other hand, if "illumination"

reaches the junction through one of the modes, say E_{A1}, we obtain the input admittance of the junction S to this wave by setting the determinant of the coefficients equal to zero and solving for $-\bar{Y}_{A1}$:

$$\begin{vmatrix} \bar{Y}_{A1} + \sum_{\mu=1}^{\infty} \alpha_{1\mu}^{\,2}\, \bar{Y}_{B\mu} & \sum_{\mu=1}^{\infty} \alpha_{1\mu}\, \alpha_{2\mu}\, \bar{Y}_{B\mu} \cdots \\ \sum_{\mu=1}^{\infty} \alpha_{1}\, \alpha_{2}\, \bar{Y}_{B} & \bar{Y}_{A2} + \sum_{\mu=1}^{\infty} \alpha_{2\mu}^{\,2}\, \bar{Y}_{B\mu} \cdots \\ \cdots\cdots\cdots\cdots\cdots\cdots\cdots\cdots & \end{vmatrix} = 0 \qquad (13)$$

Alternately we can obtain the following equation:

$$\begin{vmatrix} \bar{Z}_{B1} + \sum_{\mu=1}^{\infty} \alpha_{1\mu}^{\,2}\, \bar{Z}_{A\mu} & \sum_{\mu=1}^{\infty} \alpha_{1\mu}\, \alpha_{2\mu}\, \bar{Z}_{A\mu} \cdots \\ \sum_{\mu=1}^{\infty} \alpha_{1\mu}\, \alpha_{2\mu}\, \bar{Z}_{A\mu} & \bar{Z}_{B2} + \sum_{\mu=1}^{\infty} \alpha_{2\mu}^{\,2}\, \bar{Z}_{A\mu} \cdots \\ \cdots\cdots\cdots\cdots\cdots\cdots\cdots\cdots & \end{vmatrix} = 0 \qquad (14)$$

Approximate solutions based on these two optional equations are equivalent only if consistently a larger number of modes is taken into account in system B than in system A. This means that (13) gives a lower-order determinant than (14), but that the former requires a larger number of terms in the summations than the latter. The former is obviously easier to handle algebraically.

If (13) and (14) are written with the following shorter notation

$$\begin{vmatrix} \gamma_1 + \eta_{11} & \eta_{12} & \eta_{13} & \cdots \\ \eta_{12} & \gamma_2 + \eta_{22} & \eta_{23} & \cdots \\ \eta_{13} & \eta_{23} & \gamma_3 + \eta_{33} & \cdots \\ \cdots & \cdots & \cdots & \cdots \end{vmatrix} = 0 \qquad (15)$$

the first approximation to the solution for $-\gamma_1$ is

$$-\gamma_1 \cong \eta_{11} \qquad (16)$$

The second approximation is

$$-\gamma_1 \cong \eta_{11} - \frac{\eta_{12}^2}{\gamma_2 + \eta_{22}} \cdot \qquad (17)$$

The third approximation is

$$-\gamma_1 \cong \eta_{11} - \frac{\eta^2_{12}}{\gamma_2 + \eta_{22}} - \frac{\eta^2_{13}}{\gamma_3 + \eta_{33}} + \frac{2\eta_{12}\,\eta_{13}\,\eta_{23}}{\gamma_2\gamma_3}\,, \qquad (18)$$

where in the denominators of the second and third term η^2_{23} has been neglected in comparison with $(\gamma_2 + \eta_{22})\ (\gamma_3 + \eta_{33})$ and in the fourth term only $\gamma_2\,\gamma_3$ has been retained of this product. Higher-order approximations can easily be constructed in a similar way. In terms of the wave admittances the last equation can be written:

$$-\bar{Y}_{A1} = \sum_{\mu=1}^{\infty} \alpha_{\mu 1}\,\bar{Y}_{B\mu} - \frac{\left[\sum_{\mu=1}^{\infty} \alpha_{\mu 1}\,\alpha_{\mu 2}\,\bar{Y}_{B\mu}\right]^2}{\bar{Y}_{A2} + \sum_{\mu=1}^{\infty} \alpha_{\mu 2}^{\,2}\,\bar{Y}_{B\mu}} -$$

$$- \frac{\sum_{\mu=1}^{\infty} \alpha_{\mu 1}\,\alpha_{\mu 3}\,\bar{Y}_{B\mu}^{\,2}}{\bar{Y}_{A3} + \sum_{\mu=1}^{\infty} \alpha_{\mu 3}^{\,2}\,\bar{Y}_{B\mu}} +$$

$$+\frac{2\sum_{\mu=1}^{\infty}\alpha_{\mu 1}\alpha_{\mu 2}\bar{Y}_{B\mu}\cdot\sum_{\mu=1}^{\infty}\alpha_{\mu 1}\alpha_{\mu 3}\bar{Y}_{B\mu}\sum_{\mu=1}^{\infty}\alpha_{\mu 2}\alpha_{\mu 3}\bar{Y}_{B\mu}}{\bar{Y}_{A2}\bar{Y}_{A3}} \quad . \quad (19)$$

In case of illumination from system B the desired input admittance appears in every element of the determinant (13). The choice is then between using (13) with a procedure of successive approximations or (14) with a higher-order determinant.

The mode numbers used above are quite arbitrary. The desired wave admittance can always be made to appear in the upper left-hand corner of the determinant. The formulas given here are therefore quite general, within the restrictions imposed by convergence and computational labor.

The junction can be represented by an equivalent network showing all the various wave-guide modes involved. Fig. 2 gives such a representation. The coupling elements between the modes in one guide and those in the other are ideal transformers, connected in parallel on the side corresponding to the wave guide of smaller cross section and in series on the other side, in accord with (5) and (13).

Because of the normalizing procedure the mode coefficients, $E_{A\mu}$, $H_{A\mu}$, $E_{B\nu}$, $H_{B\nu}$, do not assume the dimensions of electric or magnetic field strength. Actually, if x_1 and x_2 have the dimension length, these coefficients have the dimension voltage and current and, therefore, fit dimensionally into the equivalent network. In any circuit containing a source the wave impedance shown in the diagram will be negative and can be replaced by a voltage generator and a T or a π network.

The simplest example of a junction of the kind described here is formed by two wave guides extended along the x_3-axis with a width 2d along

x_1, one of them with a height 2a and the other with a height 2b along x_2. For TE-waves with the electric field vector parallel to the x_2-axis the following normalized wave functions at the boundary surface exist of the lowest-order x_1-distribution

$$e_{A_o} = \frac{1}{\sqrt{2ad}} \cos \frac{\pi x_1}{2d} \tag{20}$$

$$e_{A_\mu} = \frac{1}{\sqrt{ad}} \cos\mu \frac{\pi x_2}{2a} \cos \frac{\pi x_1}{2d} \quad \text{for } \mu = 2k > 0 \tag{21}$$

$$e_{A_\mu} = \frac{1}{\sqrt{ad}} \sin\mu \frac{\pi x_2}{2a} \cos \frac{\pi x_1}{2d} \quad \text{for } \mu = 2k - 1 > 0 \tag{22}$$

The coefficients $\alpha_{\mu\nu}$ are then

$$\alpha_{oo} = \sqrt{\frac{a}{b}} \tag{23}$$

$$\alpha_{\mu o} = 0 \text{ for } \mu > 0 \tag{24}$$

$$\alpha_{o\nu} = \sqrt{\frac{2a}{b}} \frac{\sin \nu \frac{\pi a}{2b}}{\nu \frac{\pi a}{2b}} \quad \text{for } \nu = 2k > 0 \tag{25}$$

$$\alpha_{o\nu} = 0 \qquad \text{for } \nu = 2k - 1 > 0 \tag{26}$$

$$\alpha_{\mu\nu} = \sqrt{\frac{a}{b}} \qquad \text{for } \frac{\nu b}{\mu a} = 2k - 1 > 0 \tag{27}$$

$$\alpha_{\mu\nu} = 0 \qquad \text{for } \mu - \nu = 2k - 1 > 0 \tag{28}$$

If μ and ν are not related according to (27) or (28)

$$\alpha_{\mu\nu} = \sqrt{\frac{a}{b}} \left\{ \frac{\sin\left(\mu + \nu\frac{b}{a}\right) \cdot \frac{\pi}{2}}{\left(\mu + \nu\frac{b}{a}\right) \cdot \frac{\pi}{2}} + \frac{\sin\left(\mu - \nu\frac{b}{a}\right) \frac{\pi}{2}}{\left(\mu - \nu\frac{b}{a}\right) \frac{\pi}{2}} \right\} \text{for} \begin{cases} \mu = 2k > 0 \\ \nu = 2n > 0 \end{cases} \tag{29}$$

$$\alpha_{\mu\nu} = \sqrt{\frac{a}{b}} \left\{ \frac{\sin\left(\mu - \nu\frac{b}{a}\right)\cdot\frac{\pi}{2}}{\left(\mu - \nu\frac{b}{a}\right)\cdot\frac{\pi}{2}} - \frac{\sin\left(\mu + \nu\frac{b}{a}\right)\cdot\frac{\pi}{2}}{\left(\mu + \nu\frac{b}{a}\right)\cdot\frac{\pi}{2}} \right\} \quad \text{for} \begin{cases} \mu = 2k - 1 > 0 \\ \nu = 2n - 1 > 0 \end{cases} \tag{30}$$

If the widths rather than the heights of the two guides differ, analogous expressions are obtained. The zero modes are in general excluded, except for radial transmission in cylindrical structures and similar cases, and the symmetry conditions (even and odd limitations on μ and ν) are reversed, because the transverse electric field vanishes at integration boundaries instead of having a maximum there.

This analysis of discontinuities in wave guides can easily be extended to obstacles cylindrical with respect to the wave-guide axis by means of symmetry considerations. The obstacle forms a short section of wave guide of reduced cross section. Let us suppose that only one mode is propagated in the larger wave guide. Two idealized problems are solved first, and then any practical case is obtained by superposition of the two ideal solutions multiplied by proper constants.

In the first idealized problem the obstacle is illuminated from both sides by waves of equal amplitude and phase in the propagated mode. The input impedance $\overline{Z}_I$ is obtained from (14) by multiplying each $\overline{Z}_{A\mu}$ by $\cot\frac{\pi l}{\lambda_\mu}$ where $2l$ is the axial length of the obstacle and λ_μ the wave-guide wave length of the μth mode in the smaller "wave guide" formed by the obstacle.

The second idealized problem differs from the first one only by the reversed phase of illumination to the right, so that the reansverse field components are anti-symmetrical rather than symmetrical; the wave impedances $\overline{Z}_{A\mu}$ are then modified by $\tan\frac{\pi l}{\lambda_\mu}$, and an input impedance Z_{11} is determined from (14).

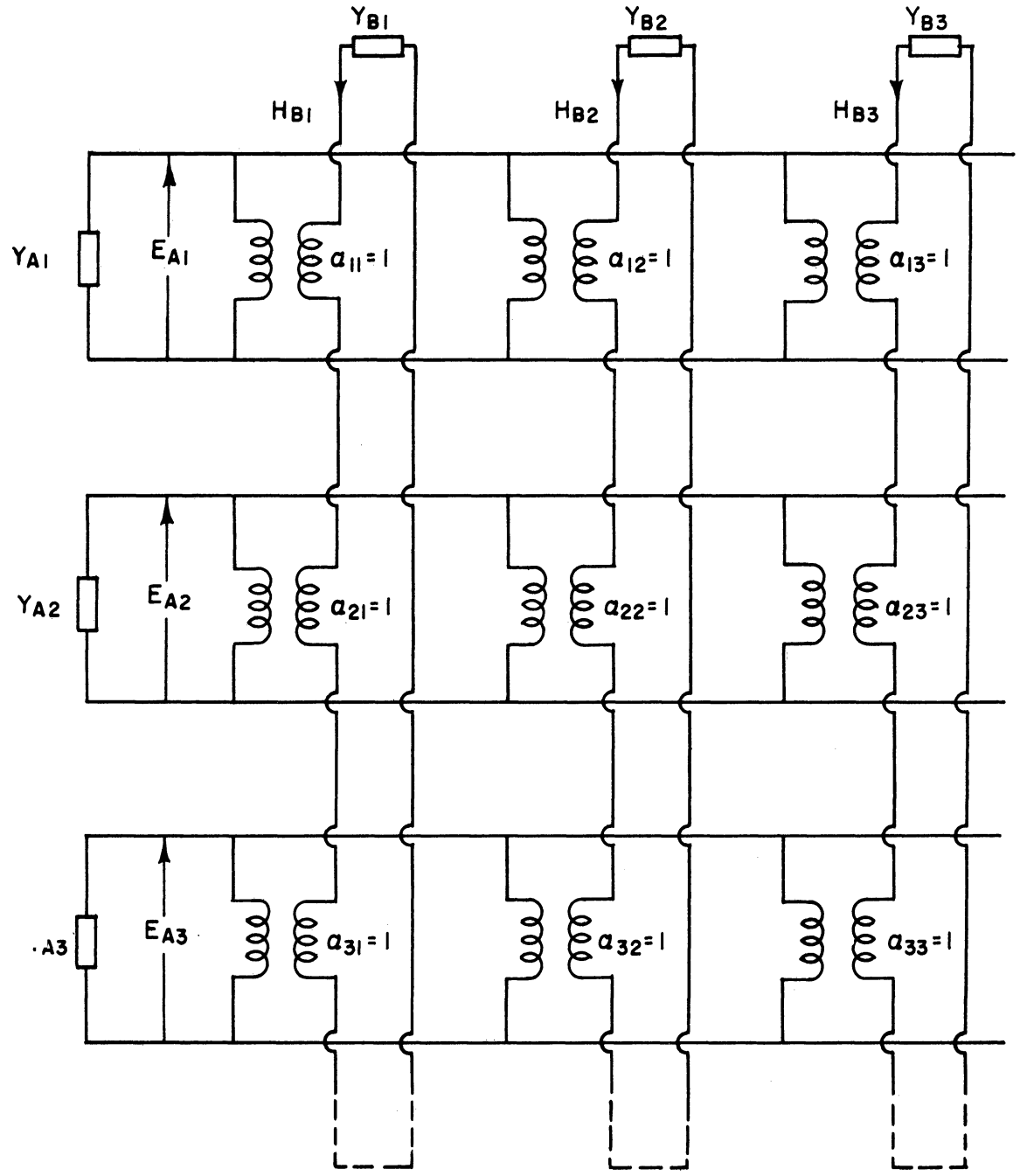

FIG. 2

EQUIVALENT NETWORK OF THE JUNCTION OF TWO WAVE GUIDES. (THE BOUNDARY SURFACE EQUAL TO THE CROSS SECTION OF THE SMALLER GUIDE).

For non-propagating modes λ_μ is imaginary and the trigonometric functions change to hyperbolic functions.

The two problems are equivalent to placing a sheet of infinite or zero impedance, respectively, at the midplane of the obstacle.[6,7]

The two solutions are added in such a way that the boundary conditions at the source and at the termination of the wave guide B are satisfied.

If more than one mode in the wave guide propagate at the frequency of excitation, ideal solutions are determined for all combinations of symmetrical and antisymmetrical illumination and all the resulting solutions are used to satisfy the boundary conditions.

Fig. 3 shows an equivalent network of a wave guide containing an obstacle cylindrical with respect to the wave-guide axis. It is seen to be derived directly from the network shown in Fig. 2.

The impedances $\bar{Z}_I$ and $\bar{Z}_{II}$ are simply related to the open-circuit and short-circuit impedances used in lumped-constant network theory, and to the elements of an equivalent T network.

If the electric field of the propagated mode in the output side of the obstacle is $E_I + h \cdot E_{II}$ and the wave impedance $\bar{Z}_2$, the factor h is determined by

$$\frac{E_2}{H_2} = \frac{E_I + h\, E_{II}}{H_I + h\, H_{II}} = \bar{Z}_2 \quad , \tag{31}$$

which reduces to

$$h = - \frac{\bar{Z}_I + \bar{Z}_2}{\bar{Z}_{II} + \bar{Z}_2} \cdot \frac{H_I}{H_{II}} \quad . \tag{32}$$

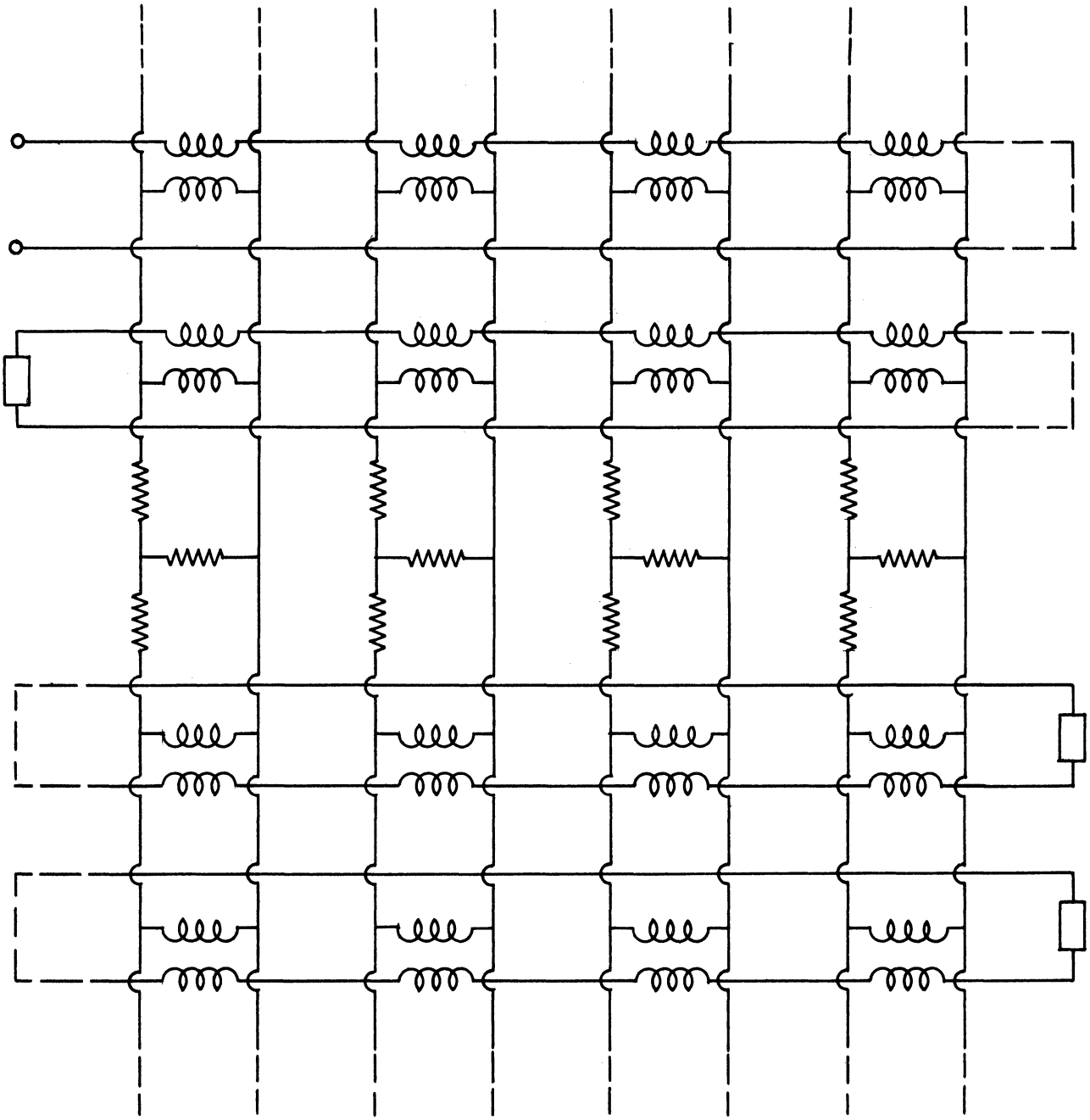

FIG. 3
EQUIVALENT NETWORK OF AN
OBSTACLE IN A WAVE GUIDE

The input impedance for the propagated mode is

$$\bar{Z}_1 = -\frac{E_I - h E_{II}}{H_I - h H_{II}} \tag{33}$$

$$= \frac{\bar{Z}_2 (\bar{Z}_I + \bar{Z}_{II}) + 2\bar{Z}_I \bar{Z}_{II}}{\bar{Z}_I + \bar{Z}_{II} + 2\bar{Z}_2} \tag{34}$$

The open-circuit and short-circuit impedances are then

$$\bar{Z}_{oc} = \frac{\bar{Z}_I + \bar{Z}_{II}}{2} \tag{35}$$

$$\bar{Z}_{sc} = \frac{2\bar{Z}_I \bar{Z}_{II}}{\bar{Z}_I + \bar{Z}_{II}} \tag{36}$$

The impedances of the equivalent T-network are

$$\begin{cases} \bar{Z}_a = \bar{Z}_I & (37) \\ \bar{Z}_b = \frac{\bar{Z}_{II} - \bar{Z}_I}{2} & (38) \end{cases}$$

$$\text{or} \begin{cases} \bar{Z}_a = \bar{Z}_{II} & (39) \\ \bar{Z}_b = \frac{\bar{Z}_I - \bar{Z}_{II}}{2} & (40) \end{cases}$$

The same procedure leads to corresponding admittance relations if we start out from (13) or (19). A simpler determinant is obtained in this case, but the desired input admittance appears in every element of the determinant. It should be emphasized again that (13) and (14) are equivalent and realistic only if we consistently account for a considerably larger number of modes in the larger cross section.

General Case $A \neq S \neq B$

In order to apply a similar procedure as used previously we introduce a set of orthogonal functions $e_{S\nu}$ over the common boundary surface S. Writing the corresponding systems of equations in a shorter notation we have

$$E_{A\mu} = \sum_{\nu=1}^{\infty} \alpha_{\mu\nu} E_{S\nu} \tag{41}$$

$$-H_{S\mu} = \sum_{\nu=1}^{\infty} \alpha_{\nu\mu} H_{A\nu} \tag{42}$$

$$\alpha_{\mu\nu} = \int_S e_{A\mu} e_{S\nu} dx_1 dx_2 \tag{43}$$

$$H_{A\mu} = E_{A\mu} \bar{Y}_{A\mu} \tag{44}$$

Similarly

$$E_{B\mu} = \sum_{\nu=1}^{\infty} \beta_{\mu\nu} E_S \tag{45}$$

$$H_{S\mu} = \sum_{\nu=1}^{\infty} \beta_{\mu\nu} H_B \tag{46}$$

$$\beta_{\mu\nu} = \int_S e_{B\mu} e_{S\nu} dx_1 dx_2 \tag{47}$$

$$H_{B\mu} = E_B \cdot \bar{Y}_{A\mu} . \tag{48}$$

In this case it is convenient to eliminate all field components except the set E_S, which forms a complete system of homogeneous linear equations for which the compatibility relation is obtained by setting the determinant

$$\left| \sum_{\mu=1}^{\infty} (\alpha_{\mu m}\, \alpha_{\mu n}\, \bar{Y}_{A\mu} + \beta_{\mu m}\, \beta_{\mu n}\, Y_{B\mu}) \right| = 0, \tag{49}$$

where the subscript n refers to the row and m to the column in the determinant. Note that the mode-number symbols μ, ν, m, n here and below are used indicriminately, since the wave system in each case is indicated by subscripts A, B, S.

In an approximate solution of this equation the number of terms in the summations should be considerably larger than the order of the determinant. Unfortunately the unknown admittance appears in all the elements of the determinant. In many practical cases it will be found expedient to obtain a first approximation by setting the upper left corner element = 0 and use the resulting admittance value in all the other elements when the higher-order approximations are calculated.

If the final system of equations instead is made to contain the components $E_{B\mu}$ the compatibility equation becomes

$$\left| \beta_{mn}\, \bar{Y}_{Bm} + \sum_{\nu=1}^{\infty} \beta_{m\nu} \sum_{\mu=1}^{\infty} \alpha_{\mu n}\, \alpha_{\mu\nu}\, \bar{Y}_{A\mu} \right| = 0, \tag{50}$$

where A and α can be interchanged with B and β because of the symmetry of the problem. Here the unknown admittance appears in the elements of one column only, but for the same accuracy a determinant of higher order has to be used. The use of (49) is, therefore, in general more convenient.

The first approximation obtained from (49) is

$$-\bar{Y}_{A1}^{(1)} = \frac{1}{\alpha_{11}^{2}}\left\{\beta_{11}^{2}\bar{Y}_{B1} + \sum_{\mu=2}^{\infty}(\alpha_{\mu 1}^{2}\bar{Y}_{A\mu} + \beta_{\mu 1}^{2}\bar{Y}_{B\mu})\right\} . \quad (51)$$

The second approximation is

$$-\bar{Y}_{A1}^{(2)} = -\bar{Y}_{A1}^{(1)} + \frac{\sum_{\mu=1}^{\infty}(\alpha_{\mu 1}\alpha_{\mu 2}\bar{Y}_{A} + \beta_{\mu}\beta_{\mu 2}\bar{Y}_{B})^{2}}{\sum_{\mu=1}^{\infty}(\alpha_{\mu}^{2}\bar{Y} + \beta_{\mu 2}^{2}\bar{Y})} . \quad (52)$$

The special case $A = B$, $\alpha = \beta$ represents an infinitely thin iris in a wave guide; a problem, however, that has been more conveniently solved by other methods.

B. A PROBLEM INVOLVING THREE-DIMENSIONAL HARMONIC ANALYSIS

A common example of a junction where the boundary surface between the two systems is not the same if described by the two relations $x_3 =$ constant and $y_3 =$ constant is shown in Fig. 4. A rectangular wave guide is opening directly into a cavity formed by a rotational cylinder or a sector of such a cylinder. The height $2h_G$ of the wave guide is smaller than the axial height $2h_C$ of the cavity. The same coordinate $y_2 = y_2 = y$ can be used in this dimension, but the other coordinates, $y_1 = \varphi$, $y_3 = r$ and $x_1 = -x$, $x_3 = z$ are different in the two systems. It is evidently convenient in this case to place the origin of both coordinate systems on the axis of the cylinder rather than on the boundary surface. As a consequence the wave admittance for waves traveling in the negative direction is calculated from the transverse field components with the sign of the magnetic field reversed. In order to apply as far as possible the same

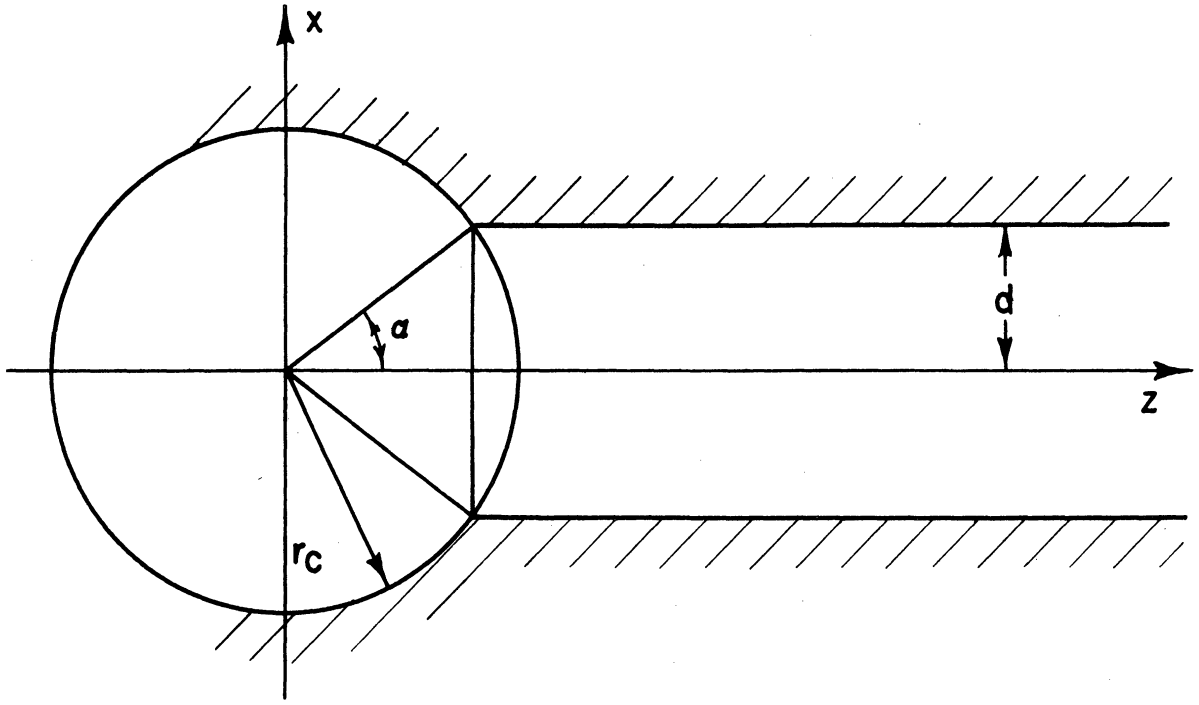

FIG. 4
JUNCTION OF A CYLINDRICAL CAVITY
AND A RECTANGULAR WAVE GUIDE

procedure here as in previous problems we shall consider the cavity as a wave guide with wave propagation in radial direction.

We can formulate boundary conditions either at the surface $r = r_c$ or at the surface $z = r_c$, but before this can be done in the same way as before, the field components must be expressed in terms of the same kind of waves, plane or cylindrical, on both sides of the boundary. Let us, for instance, translate the plane-wave field components in the wave guide to cylindrical-wave field components and then introduce the boundary conditions at the surface $r = r_c$. This problem of expanding the plane waves into cylindrical waves can be attacked in more than one way. We would like to have the azimuthal wave functions form an orthogonal set over the wave-guide opening rather than over 2π, so that only one more expansion, in terms of the modes of the cylindrical cavity, would be required to solve the problem in accordance with the two-dimensional procedure previously presented. However, this would in general lead to cylinder functions of nonintergral order and very awkward integration limits for calculation of the coefficients in the series. The computational problem would be, for all practical purposes, prohibitive.

A more reasonable alternative involves extrapolation of the wave-guide waves to infinite plane waves, translating these to cylindrical waves expressible in integral-order cylinder functions. Two subsequent two-dimensional expansions are then required, one in terms of orthonormal functions over the curved surface $r= r_c$ limited by the wave guide opening, and the other identical to the set of normal modes in the cavity. Thus we buy the more easily computable three-dimensional expansion at the cost of performing an additional two-dimensional expansion and summation.

The purpose of the three-dimensional expansion is to express the cavity-mode components, E_y and $H\varphi$ at the boundary surface $r = r_c$ in terms of the complex amplitudes of the wave-guide modes.

Waves propagated in the opposite directions are orthogonal in three-dimensional space and can, therefore, not as conveniently as in the two-dimensional analysis be lumped together and their relation expressed by a wave admittance. We shall here express the amplitude of a wave propagated in the negative z-direction as equal to the one of the positive wave multiplied by a complex reflection coefficient ρ, referred to the origin, $z = 0$.

Using as before small letters e and h for wave functions and introducing the subscript G for the plane waves and A for the cylindrical waves as will as superscripts (1) and (2) to indicate positive and negative direction of propagation, respectively, we obtain the following equations for the above field components in space:

$$E_y = \sum_{\mu} E_{G\mu} \left[e_{G\mu}^{(1)}(z) + \rho_{\mu}\, e_{G\mu}^{(2)}(z) \right] e_{G\mu}(x, y) \tag{53}$$

$$E_y = \sum_{\nu} E_{A\nu} \left[e_{A\nu}^{(1)}(r) + \rho_{\nu}\, e_{A\nu}^{(2)}(r) \right] e_{A\nu}(\varphi, y) \tag{54}$$

$$H_{\varphi} = \sum_{\nu} E_{A\nu} \cdot Y_o \left[h_{A\nu}^{(1)}(r) + f(\rho_{\nu})\, h_{A\nu}^{(2)}(r) \right] h_{A\nu}(\varphi, y). \tag{55}$$

As before Y_o is the wave admittance of free space $\sqrt{\epsilon_o/\mu_o}$.

The relations between plane wave functions and cylindrical wave functions can be written

$$e_{G\mu}(x, z, y) = \sum_{\nu} \alpha_{\nu\mu}\, e_{A\nu}(r, \varphi, y) \tag{56}$$

$$h_{Av}(r, \varphi, y) = \phi\left[e_{Av}(r, \varphi, y)\right] . \tag{57}$$

The last equation, where $\phi[\,]$ stands for "function of", is based on the fact that all vector components of a circularly cylindrical wave can be derived from the wave functions of one and the same scalar quantity.

Introducing the subscript B for field components of the cylindrical waves at the boundary $r = r_c$ we get from (53) to (57)

$$\sum_{v} E_{Bv}\, e_{Av}(\varphi, y) = \sum_{v} E_{Av}\left[e_{Av}^{(1)}(r_c) + \rho_v\, e_{Av}^{(2)}(r_c)\right] e_{Av}(\varphi, y)$$

$$= \sum_{\mu} E_{G\mu} \sum_{v} a_{v\mu}\, e_{Av}(\varphi, y) \tag{58}$$

$$\sum_{v} H_{Bv}\, e_{Av}(\varphi, y) = \sum_{v} E_{Av}\, Y_o\left[h_{Av}^{(1)}(r_c) + f(\rho_v)\, h_{Av}^{(2)}(r_c)\right] h_{Av}(\varphi, y)$$

$$= \sum_{\mu} E_{G\mu}\, Y_o \sum_{v} b_{v\mu}\, e_{Av}(\varphi, y) \quad , \tag{59}$$

where we have introduced for short

$$a_{v\mu} = \alpha_{v\mu}^{(1)}\, e_{Av}^{(1)}(r_c) + \rho_\mu\, \alpha_{v\mu}^{(2)}\, e_{Av}^{(2)}(r_c) \tag{60}$$

$$b_{v\mu} = \alpha_{v\mu}^{(1)}\, h_{A}^{(1)}(r_c) + f(\rho_\mu)\, \alpha_{v\mu}^{(2)}\, h_{Av}^{(2)}(r_c) \tag{61}$$

$$e_{Av}(\varphi, y) = h_{Av}(\varphi, y) \quad . \tag{62}$$

The analytic expressions for the cylindrical wave functions and the coefficients of coupling will be given later.

Following the procedure in previous sections we can rewrite (58) and (59) as the following linear systems of equations between the coefficients in the expansions

$$E_{B\nu} = \sum_{\mu} a_{\nu\mu} E_{G\mu} \tag{63}$$

$$H_{B\nu} = \sum_{\mu} b_{\nu\mu} Y_o E_{G\mu} \cdot \tag{64}$$

From here on we apply the two-dimensional analysis presented in previous sections. If the subscripts S and C refer to the coefficients of the orthogonal wave functions over the common boundary at $r = r_c$ and over the whole cavity circumference, respectively, the following additional systems of equations are obtained

$$E_{S\zeta} = \sum_{\nu} \gamma_{\nu\zeta} E_{B\nu} \tag{65}$$

$$H_{S\zeta} = \sum_{\nu} \gamma_{\nu\zeta} H_{B\nu} \tag{66}$$

$$E_{C\xi} = \sum_{\zeta} \eta_{\xi\zeta} E_{S\zeta} \tag{67}$$

$$H_{S\zeta} = \sum_{\xi} \eta_{\xi\zeta} H_{C\xi} = \sum_{\xi} \eta_{\xi\zeta} E_{C\xi} (-\bar{Y}_{C\xi}) \cdot \tag{68}$$

where

$$\gamma_{\mu\nu} = \int_{-\alpha}^{+\alpha} \int_{-h_G}^{+h_G} e_{A\mu}(\varphi, y)\, e_{S\nu}(\varphi, y)\, d\varphi\, dy$$

$$\gamma_{\mu\nu} = \int_{-h_G}^{+h_G} e_A(y)\, e_S(y)\, dy \frac{1}{\sqrt{\pi\alpha}} \int_{-\alpha}^{+\alpha} \cos\mu\varphi \cos\frac{\pi_\nu \varphi}{2\alpha} d\varphi \qquad (69)$$
$$(\nu \text{ odd})$$

For even values of ν the cosines should be replaced by sines. For $\mu = 0$ the right member should be multiplied by $1/\sqrt{2}$.

The corresponding coefficients on the cavity side differ only by the variation of the wave functions with y.

$$\eta_{\mu\nu} = \int_{-\alpha}^{+\alpha} \int_{-h_G}^{+h_G} e_{G\mu}(\varphi, y)\, e_{S\nu}(\varphi, y)\, d\varphi\, dy \quad . \qquad (70)$$

Elimination of $E_{C\xi}$ between (67) and (68) gives

$$H_{S\xi} = \sum_X (-\bar{Y}_{S\xi X})\, E_{SX} = \sum_X E_{SX} \sum_\xi \eta_{\xi X}\, \eta_{\xi\xi}\, (-\bar{Y}_{C\xi}) \quad . \qquad (71)$$

Continued elimination leads to a homogeneous system of equations in E_G with the compatibility determinant equation

$$\left| \sum_\nu a_{\nu\mu} \sum_X \gamma_{\nu X} \cdot \bar{Y}_{SX\xi} + Y_o \sum_\nu \gamma_{\nu\xi}\, b_{\nu\mu} \right| = 0 \qquad (72)$$

This is the relation between the wave admittances of the cavity modes, implicit in the admittances $\bar{Y}_S$ defined by (71), and the reflection

coefficients in the wave guide, implicit in a and b according to (60) and (61). (72) can only be satisfied by non-vanishing fields if at least one reflection coefficient has an absolute value larger than one or at least one of the wave admittances in the cavity has a negative real part.

In order to compute a first approximation of the input admittance of the junction we reduce the determinant to the corner element representing the lowest-order mode in the waveguide and also limit the summations over the waveguide opening (subscripts $\varkappa$ and ζ) to one term. The result can be written

$$-\bar{Y}_{S11} = Y_o \frac{\sum_{\nu} b_{\nu 1} \gamma_{\nu 1}}{\sum_{\nu} a_{\nu 1} \gamma_{\nu 1}} \qquad (73)$$

The most important element in the equivalent circuit of the junction is the turn ratio of the ideal transformer between the dominant wave guide mode and the resonant cavity mode, because the "impedance match" between the two modes depends primarily on this ratio. If the resonant mode in the cavity is the nth mode, the important term in the expansion for $\bar{Y}_{S11}$ is $\eta_{n1}^2 \cdot \bar{Y}_{Cn}$. In the right member of (73) (i.e. in (60) and (61)) the reflection coefficient ρ_1 is replaced by the wave admittance of the dominant mode at $z = r_c$ by means of the identity

$$\bar{Y}_{G1} = \frac{k_z}{k} \cdot Y_o \frac{e^{-jk_z r_c} - \rho_1 e^{jk_z r_c}}{e^{-jk_z r_c} + \rho_1 e^{jk_z r_c}} , \qquad (74)$$

where

$$k_z = k\sqrt{1 - (\lambda/4d)^2} = \frac{2\pi}{\lambda}\sqrt{1 - (\frac{\lambda}{4d})^2} \quad .$$

The approximate ratio of the ideal transformer between the two modes is then obtained as $\sqrt{-\bar{Y}_{Cn}/\bar{Y}_{Gl}}$ from (73) after these modifications.

It remains to express the coefficients $a_{\nu\mu}$ and $b_{\nu\mu}$ in terms of ordinary cylinder functions. The expansion of a plane wave into circularly cylindrical waves is well known.* The two plane waves forming a propagated TE_{no}-wave in a rectangular wave guide can be expressed in the following way

$$e_n(x, z) = q \cos k_x x e^{-jk_z z} = q \cos(kr \sin\beta_n \sin\varphi)\, e^{-jkr \cos\beta_n \cos\varphi} \qquad (76)$$

where

$$\begin{aligned} x &= r\sin\varphi \qquad k_x/k = \sin\beta_n = \frac{n\lambda}{4d} \\ z &= r\cos\varphi \qquad k_z/k = \cos\beta_n = \sqrt{1 - (\frac{n\lambda}{4d})^2} \end{aligned} \quad . \qquad (77)$$

In (76) it is not necessary to evaluate the normalizing factor q, as long as we are interested only in admittances and admittance ratios.

(76) transforms to

$$\begin{aligned} e_n(x, z) &= \frac{q}{2}\left\{e^{jkr\cos(\beta_n - \varphi)} + e^{jkr\cos(\beta_n + \varphi)}\right. \\ &= q\left\{J_o(kr) + 2\sum_{m=1}^{\infty}(-j)^m J_m(kr)\cos m\beta_n \cos m\varphi\right\}. \end{aligned} \qquad (78)$$

---

* See ref. 5 p. 371.

The wave function and corresponding expansion for propagation in the opposite direction is the complex conjugate relation to (78).

For calculation of the corresponding equation for the transverse magnetic field we make use of the relation between the transverse components in a cylindrical TM-wave (Eq. (5) in part II of this paper):

$$h_{An}(r,\varphi) = -j \frac{\partial}{\partial (kr)} e_{An}(r,\varphi) \quad . \tag{79}$$

(60) and (61) thus become

$$a_{o\mu} = q \sqrt{2\pi}\, J_o (kr_c)\, (1 + \rho_\mu) \tag{80a}$$

$$a_{\nu\mu} = 2q \sqrt{\pi}.J_\nu (kr_c) \left[(-j)^\nu + \rho_\mu\, j^\nu\right] \cos \nu\, \beta_\mu \quad (\nu > 0) \tag{80b}$$

$$b_{o\mu} = jq \sqrt{2\pi}\, J_o' (kr_c)\, (1 + \rho_\mu) \tag{81a}$$

$$b_{\nu\mu} = 2jq\sqrt{\pi\, J_\nu}' (kr_c) \left[(-j)^\nu + \rho_\mu\, j^\nu\right] \cos \nu\, \beta_\mu \quad (\nu > 0) \tag{81b}$$

The extension to TE_{mn}-modes is straightforward, but it is not required for the approximate solution of the present problem.

In order to evaluate the equivalent susceptance of the junction we should also expand the attenuated modes of the wave guide in terms of cylinder functions. Since the cylinder functions form a complete orthogonal set, this can be done. However, to calculate higher-order approximate solutions of (70) is beyond the scope of this paper.

The general solution to the problem discussed in this section is contained in (72). We have shown how the constants of this equation can be evaluated {(69), (70), (60), (61), (80), and (81)} and how approximate values of the admittance of such a junction between a cylindrical cavity and a rectangular wave guide can be calculated.

CALCULATION OF A WAVE-GUIDE-LOADED RESONATOR FOR INTERDIGITAL MAGNETRONS

PART II SOLUTION OF THE SPECIFIC PROBLEM

INTRODUCTION

Since the war-time work of Crawford and Hare,[1] in which the author had the opportunity to participate to a minor extent, the interdigital magnetron has been subject to a fair amount of interest. The reason is primarily the simplicity of its resonant system, which means comparatively large mode separation and wide-range tunability. A thorough analysis of the resonance frequencies of resonators for such magnetrons has been presented by a Harvard group in a report to the Office of Naval Research.[2] Operation in the lowest-order mode has been studied at the University of Michigan.[3] A more recent paper by J. Hull[4] contains additional contributions to the analysis of interdigital magnetron resonators.

The main topic of the present paper is the impedance transformation from the wave-guide load, constituting the output terminals, to the anode segments forming the input terminals of the resonator of an interdigital magnetron. The primary objective is to present a design procedure whereby the conductance at the anode segments can be made to agree at a given resonance frequency with an optimum value specified by the electronic system. The results are not unique; it is, therefore, possible to take into account also conditions for frequency stability and

circuit efficiency. For this reason, the calculations of external and internal Q are included, and the main design parameters are discussed.

Fig. 1 shows a somewhat simplified model of an interdigital magnetron resonator, in two slightly different versions, A and B. The central cylindrical post K represents the cathode, F the finger system, i.e., the interdigital anode segments (developed in Fig. 2), I, the interaction space, C the cavity external to the fingers, T the wave-guide transformer section, and G the wave guide. The electrode system is designed for operating in the second-order azimuthal mode of the cavity, that is, the mode in which the electric field strength varies through two cycles as the coordinate φ varies from 0 to 2π. In Model A, the interaction space and the cavity are of equal axial height, so that the resonator appears as a flat cylindrical cavity with a central post and a number of fingers arranged in a circle and fixed each to one of the flat walls. In Model B, the interaction space has been extended at E in axial direction as a first approximation of the actual insulating space between anode and cathode, which because of cathode end hats, pole pieces, etc., has too complicated a geometry for close calculation. The analysis presented here starts out from the geometry of Model A; the modifications introduced by the extended interaction space are discussed later and comparisons made with the experimental data.

The design problem includes choosing a suitable matching network between the cavity and the wave guide and calculating the optimum dimensions of this network.

The main alternatives offered are a simple aperture (iris), a quarter-wave uniform wave-guide section, or a tapered wave-guide section.

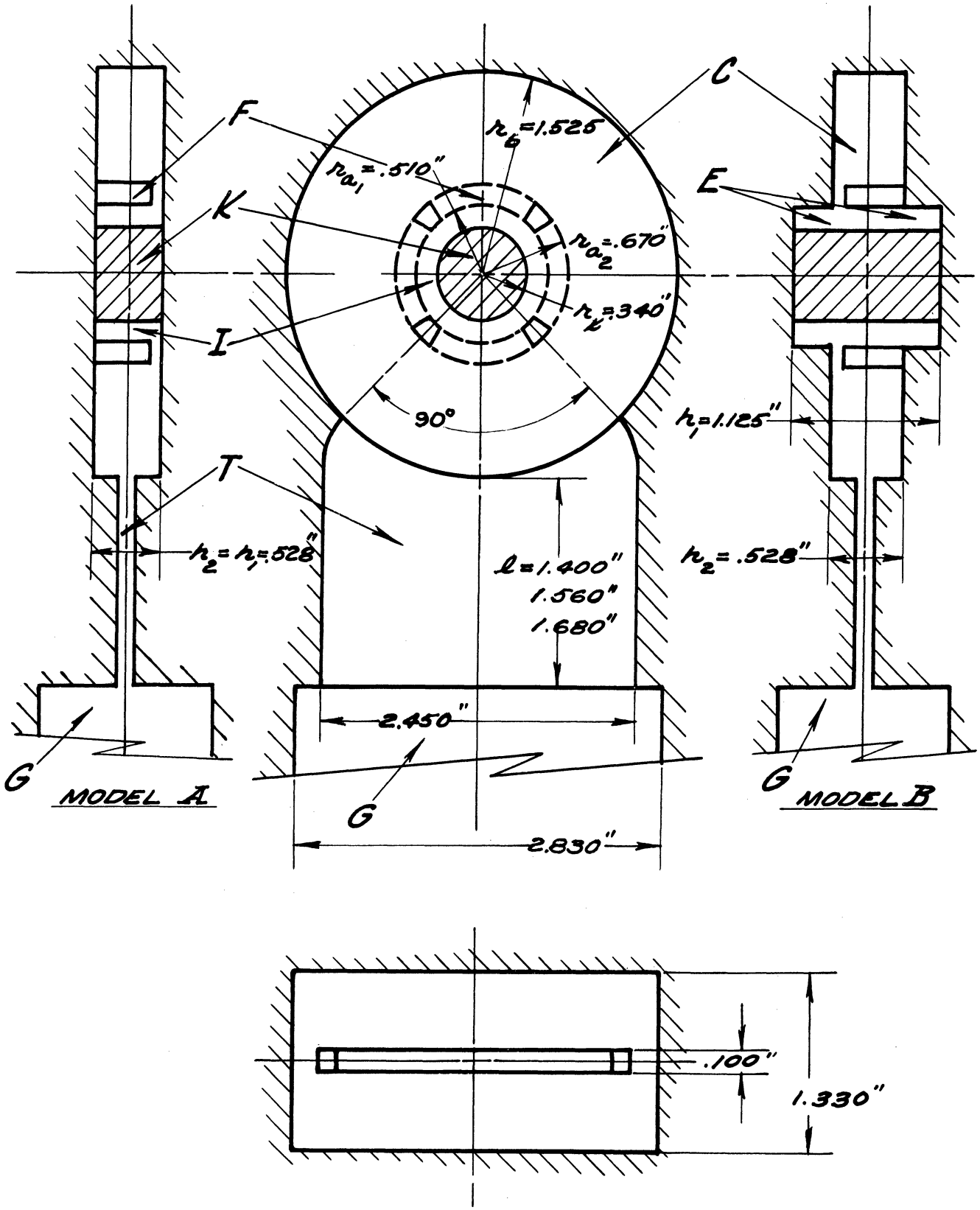

COLD TEST MODEL

FIGURE 1.

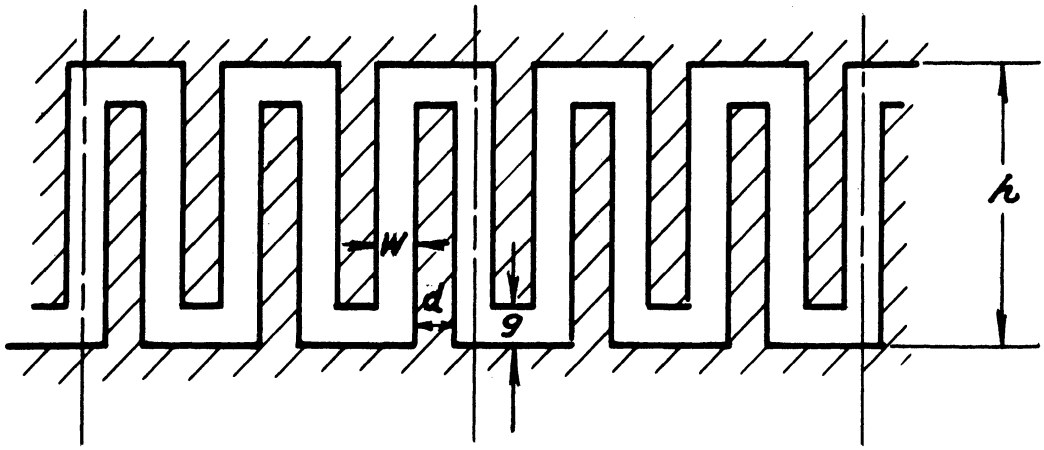

A

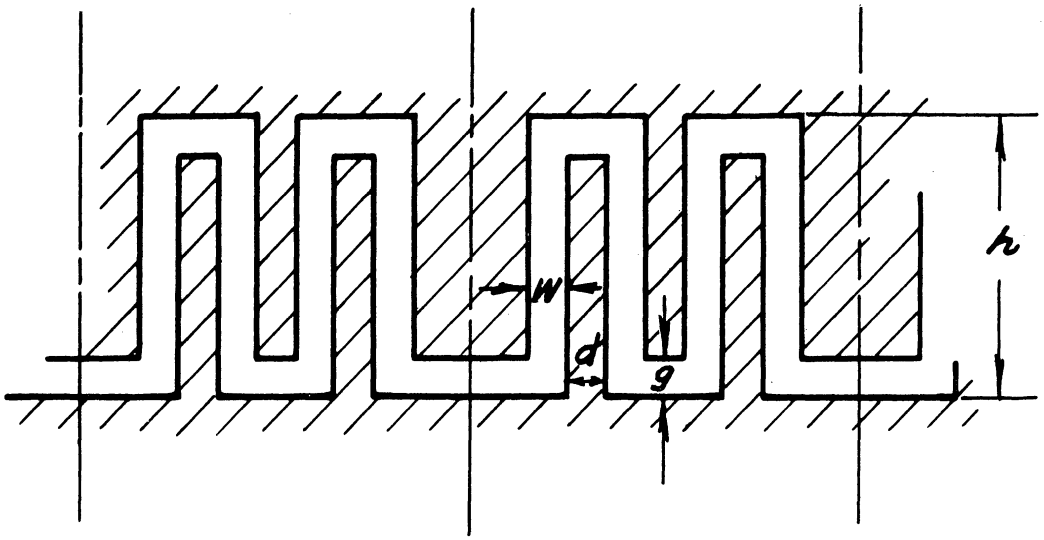

B

FIGURE 2.

The order given represents decreasing simplicity and increasing bandwidth. As a compromise solution, the second alternative has been chosen. It is undesirable to have too frequency sensitive a transducer, particularly if it may be anticipated that tunable or semitunable resonators will ultimately be desired. However, the desired bandwidth was in this case not so large as to require a tapered transformer.

Several ways of designing the transformer section are open. Fig. 3 shows: (a) a section employing cylindrical waves and forming a natural extension of the cavity, (b) a rectangular section, (c) a "ridged" or "H-shaped" section.

The first and the third of these alternatives are suitable when the cavity is small compared to the wave length. In the present design problem, the second alternative can be applied without approaching the cut-off-frequency of the transformer section too closely. The design chosen is shown in Fig. 1. It should be noted that there is no strong argument in favor of the short taper that makes the wave-guide opening exactly one quarter of the cavity circumference. On the contrary, a harmonic analyisis of the transition from cylincrical to plane waves would be somewhat simpler if the sides of the wave-guide transformer were straight all the way to the cavity.

A. ANALYSIS OF FIELD CONFIGURATION IN RESONATOR

1. Equivalent Transmission Line. Outline of Procedure.

The analysis in this paper follows the conventional procedure: the electro-magnetic field is calculated under the assumption that the conductivity of the metallic boundaries is infinite. The copper losses are subsequently obtained from the tangential component of the magnetic field so calculated and the "skin resistance" of the conductors.

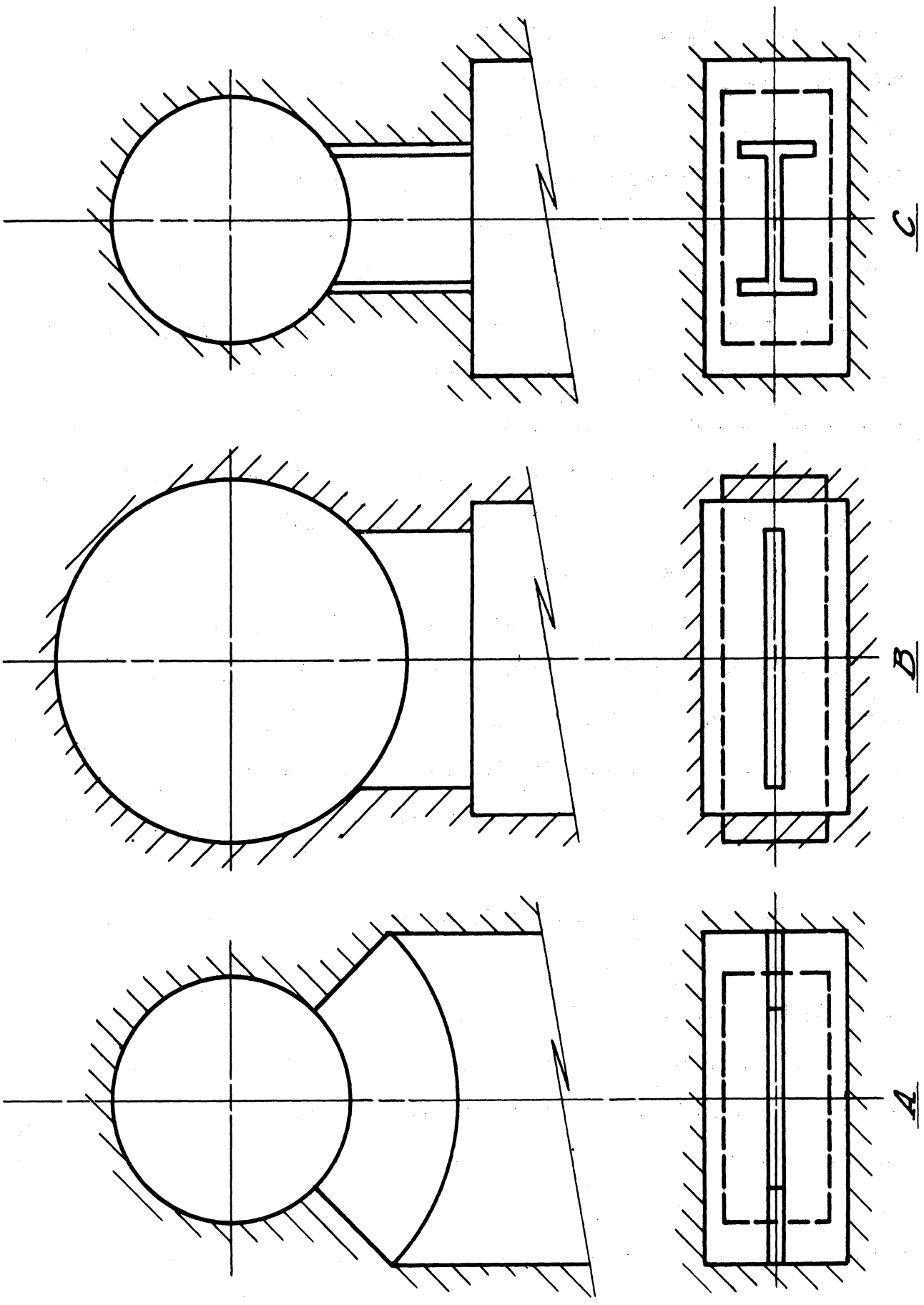

FIGURE 3.

In Fig. 4A, the resonator and its output coupling is presented as a transmission line or wave guide with a short circuit at one end (the cathode) and a number of discontinuities representing the boundaries between the interaction space and the finger system (r_{a1}), the finger system and the cavity (r_{a2}), the cavity and the transformer section (r_b), and the transformer section and the wave guide (t), respectively. In Fig. 4B, a T-junction accounts for the insulating space between the anode and the cathode structures. The modification of the calculations by consideration of this junction is particularly important when the cavity is operated in the zero-order mode, i.e., the mode with no variation of the electromagnetic field with the azimuthal coordinate . However, in this paper, we shall consider only modes of higher order, where the axial branches are operated in their cut-off range and modify the resonance frequency and energy storage only to a very moderate extent.

In the equivalent wave guide shown in Fig. 4, the characteristic impedance of the whort section F representing the finger system is very low, and since its dimension in the direction of propagation is very small compared to the wavelength, the line voltage can be considered constant between r_{a1} and r_{a2} so that the finger system acts as a lumped susceptance.

The most fundamental condition imposed on the resonator is that its resonance frequency have a specified value. This condition can conveniently be expressed as follows: at this frequency the total susceptance at any convenient phase plane, say the cylindrical surface with radius r_{a2}, should be zero. For the purpose of calculating the susceptance contributed by the various sections of the equivalent line, the sections $r_{a1} - r_k$ and $r_{a2} - r_b$ are considered short-circuited at r_k and r_b, respectively. The impedance of the transformer section at r_b is small which justifies this approximation for calculation of the susceptance alone.

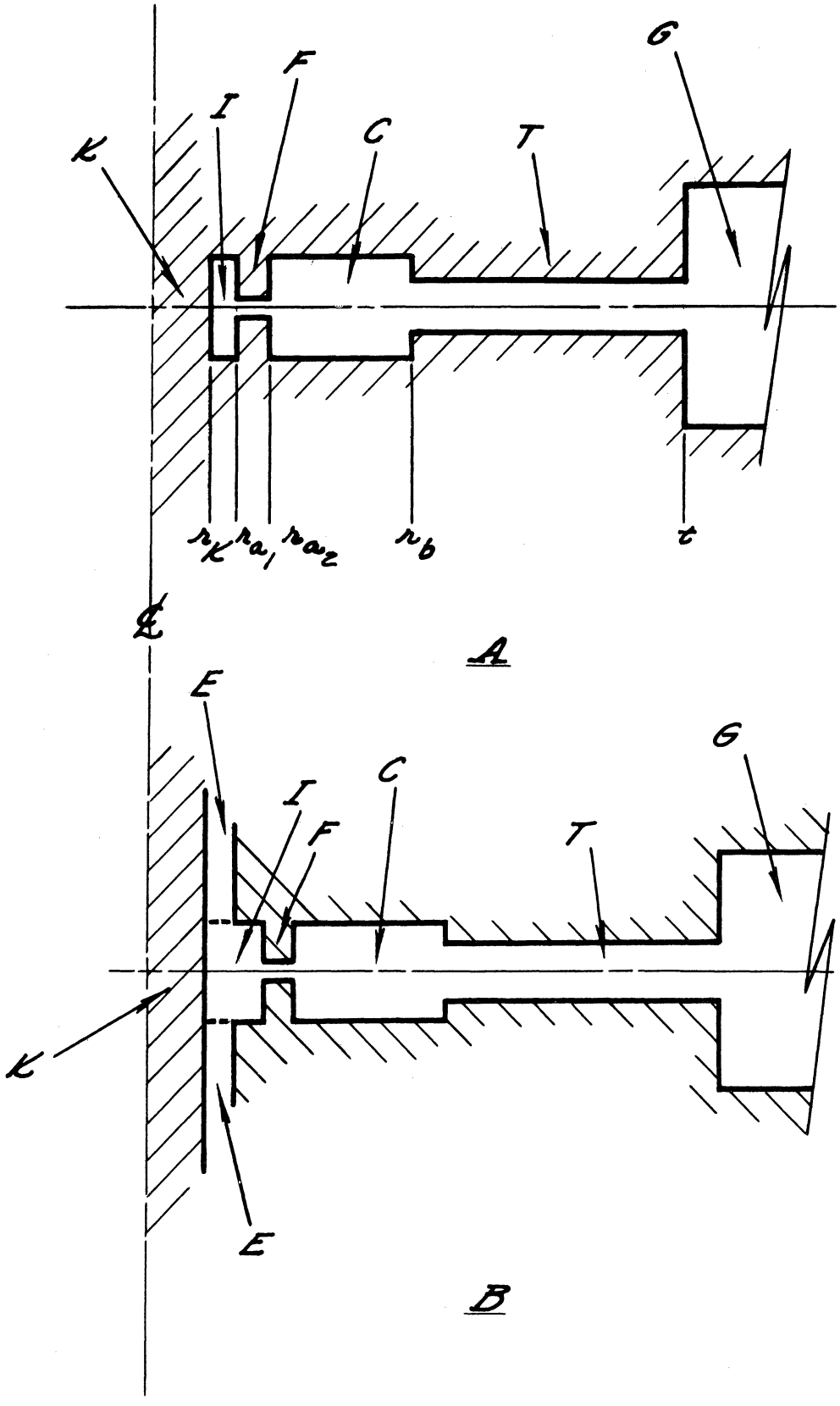

FIGURE 4.

[redacted]

$$\mathcal{H}_r = -j\frac{kn}{k_r^2 r}\mathcal{E}_o Y_o Z_n(k_r r)\sin n\varphi \tag{4}$$

$$\mathcal{H}\varphi = -j\frac{k}{k_r}\mathcal{E}_o Y_o Z'_n(k_r r)\cos n\varphi \tag{5}$$

$$\mathcal{H}_y = 0 \tag{6}$$

TE-waves:

$$\mathcal{E}_r = j\frac{kn}{k_r^2 r}\frac{\mathcal{H}_o}{Y_o} Z_n(k_r r)\sin n\varphi \tag{7}$$

$$\mathcal{E}\varphi = j\frac{k}{k_r}\frac{\mathcal{H}_o}{Y_o} Z'_n(k_r r)\cos n\varphi \tag{8}$$

$$\mathcal{E}_z = 0 \tag{9}$$

$$\mathcal{H}_r = j\frac{k_y}{k_r}\mathcal{H}_o Z'_n(k_r r)\cos n\varphi \tag{10}$$

$$\mathcal{H}\varphi = -j\frac{k_y}{k_r^2 r}\mathcal{H}_o Z_n(k_r r)\sin n\varphi \tag{11}$$

$$\mathcal{H}_y = \mathcal{H}_o Z_n(k_r r)\cos n\varphi \ , \tag{12}$$

where

$$k^2 = \frac{\omega^2}{c^2} = k_r^2 + k_y^2 \tag{13}$$

and Y_o is the admittance of free space, 2650μ mhos, $Z_n(x)$ a cylinder function of order n, $Z'_n(x) = \partial/\partial x\left[Z_n(x)\right]$. The common factor exp $(j\omega t - jk_y y)$ is considered included in $\mathcal{E}_o$ and $\mathcal{H}_o$.

and Y_o is the admittance of free space, 2650μ mhos, $Z_n(x)$ a cylinder function of order n, $Z'_n(x) = \partial/\partial x\left[Z_n(x)\right]$. The common factor exp $(j\omega t - jk_y y)$ is considered included in $\mathcal{E}_o$ and $\mathcal{H}_o$.

no variation with y ($k_y = 0$). These waves have only three field components $\mathcal{E}_y, H_r, H_\varphi$, and $k_r = k = 2\pi/\lambda$. In analogy with the exponential form of the ordinary transmission-line equations, we can express the field in terms of radially traveling waves by the use of Hankel functions.[5] Representing an inward traveling wave by a Hankel function of the first kind and an outward wave by one of the second kind, we write in general:

$$Z_n(k_r r) = A\, H_n^{(1)}(k_r r) + B\, H_n^{(2)}(k_r r) = G_n(Ae^{j\theta} + Be^{-j\theta}) \quad (14)$$

$$\begin{aligned} Z'_n(k_r r) &= A \frac{\partial}{\partial k_r r} H_n^{(1)}(k_r r) + B \frac{\partial}{\partial k_r r} H_n^{(2)}(k_r r) \\ &= j\bar{G}_n\,(-Ae^{j\psi} + Be^{-j\psi}) \quad , \end{aligned} \quad (15)$$

where the symbols G_n, $\bar{G}_n$, θ, and ψ have been introduced to represent the amplitudes and phase angles of the Hankel function and its derivative. We shall use the ratio

$$y_{or} = \frac{\bar{G}_n(k_r r)}{G_n(k_r r)} \quad (16)$$

as a normalized admittance value for radial transmission. If the cavity is terminated at $r = r_b$ by a wave admittance $\bar{Y}_b$, we "normalize" this admittance as follows

$$\eta_b = \frac{\bar{Y}_b}{y_{ob} \cdot Y_o} \quad (17)$$

If this ratio is introduced as a boundary condition in (14) and (15), the ratio between the constants A and B can be determined, and the admittance at an arbitrary radius r becomes

$$\bar{Y}_r = y_{or} \cdot Y \frac{j \sin(\psi_b - \psi) + \eta_b \cos(\theta_b - \psi)}{\cos(\psi_b - \theta) + j\eta_b \sin(\theta_b - \theta)} \quad . \tag{18}$$

This relation is of course analogous to a well-known formula for the admittance of a uniform transmission line of characteristic admittance Y_o terminated by an admittance Y_b at $x = b$

$$Y(x) = Y_o \frac{j \sin k(b - x) + Y_b/Y_o \cos k(b - x)}{\cos k(b - x) + j\, Y_b/Y_o \sin k(b - x)} \quad . \tag{19}$$

Figs. 5-9 give graphs of the quantities y_{or}, θ and ψ as functions of kr for n = 0, 1, 2, and 3.

3. The Axial Extensions of the Interaction Space

The admittance of the interaction space seen from r_{al} is obtained from (8) by reversing the direction of propagation and introducing the values θ_k and ψ_k for the cathode in place of θ_b and ψ_b

$$\bar{Y}_{al} = y_{al} \cdot Y_o \frac{\cos(\psi - \theta_k)}{j \sin(\theta - \theta_k)} \quad . \tag{20}$$

This turns out to be by far the largest inductive susceptance in the resonator. The modification of the geometry of this space by the necessary insulation between anode and cathode is consequently bound to have a considerable influence on the resonance frequency and energy storage of the resonator. In order to study the evaluation of $\bar{Y}_{al}$ in a geometry thus modified, let us consider the configuration shown as Model B in Fig. 1. The change in axial height that takes place at $r = r_{al}$ results in a rather complicated (i.e., analytically complicated) field which for an exact description requires an infinite expansion in both

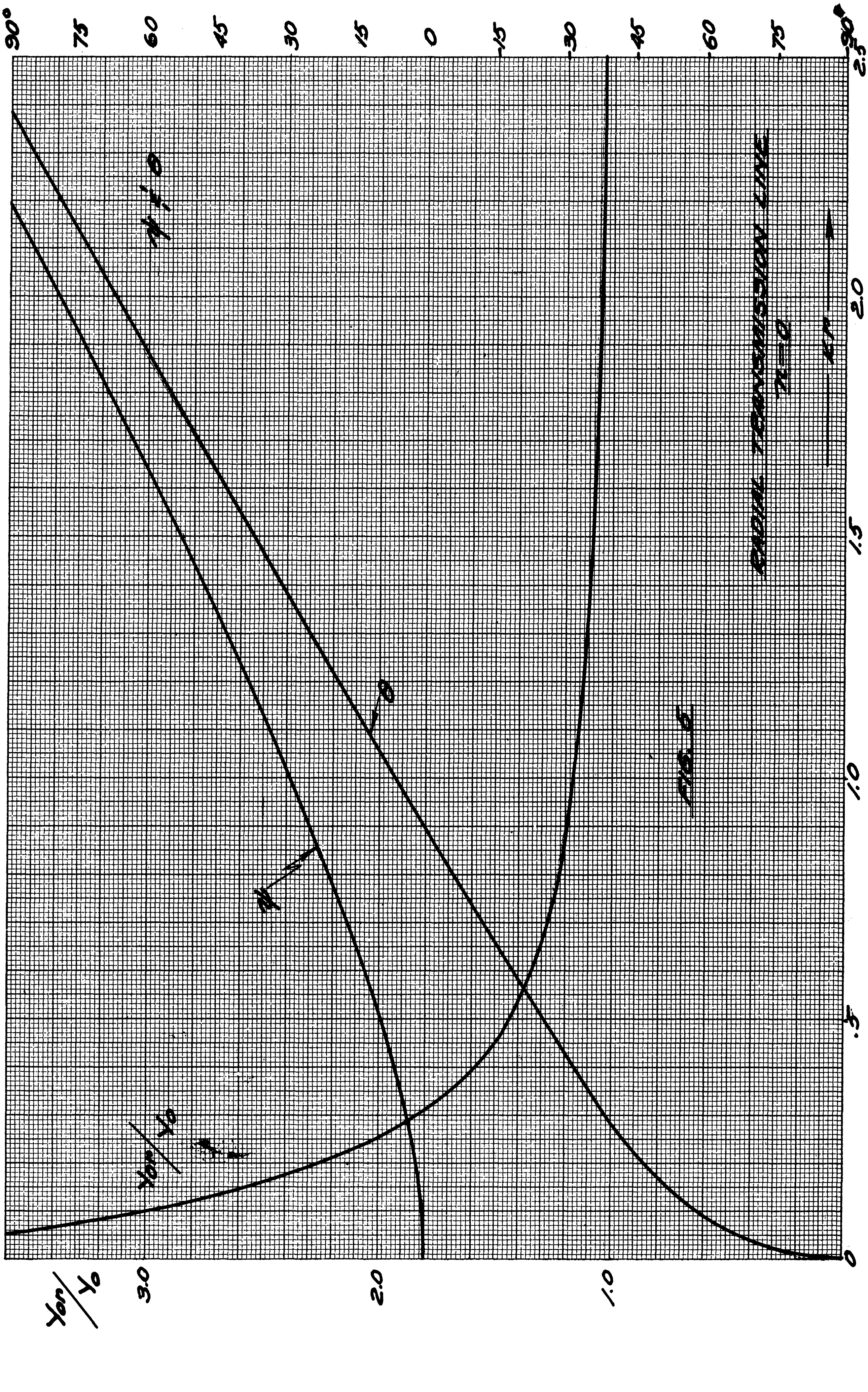
RADIAL TRANSMISSION LINE
n=0
FIG. 6
kr
Yon/Yo
ψ-θ
θ
ψ
90°
75
60
45
30
15
0
15
30
45
60
75
90°
3.0
2.0
1.0
0
.5
1.0
1.5
2.0
2.5

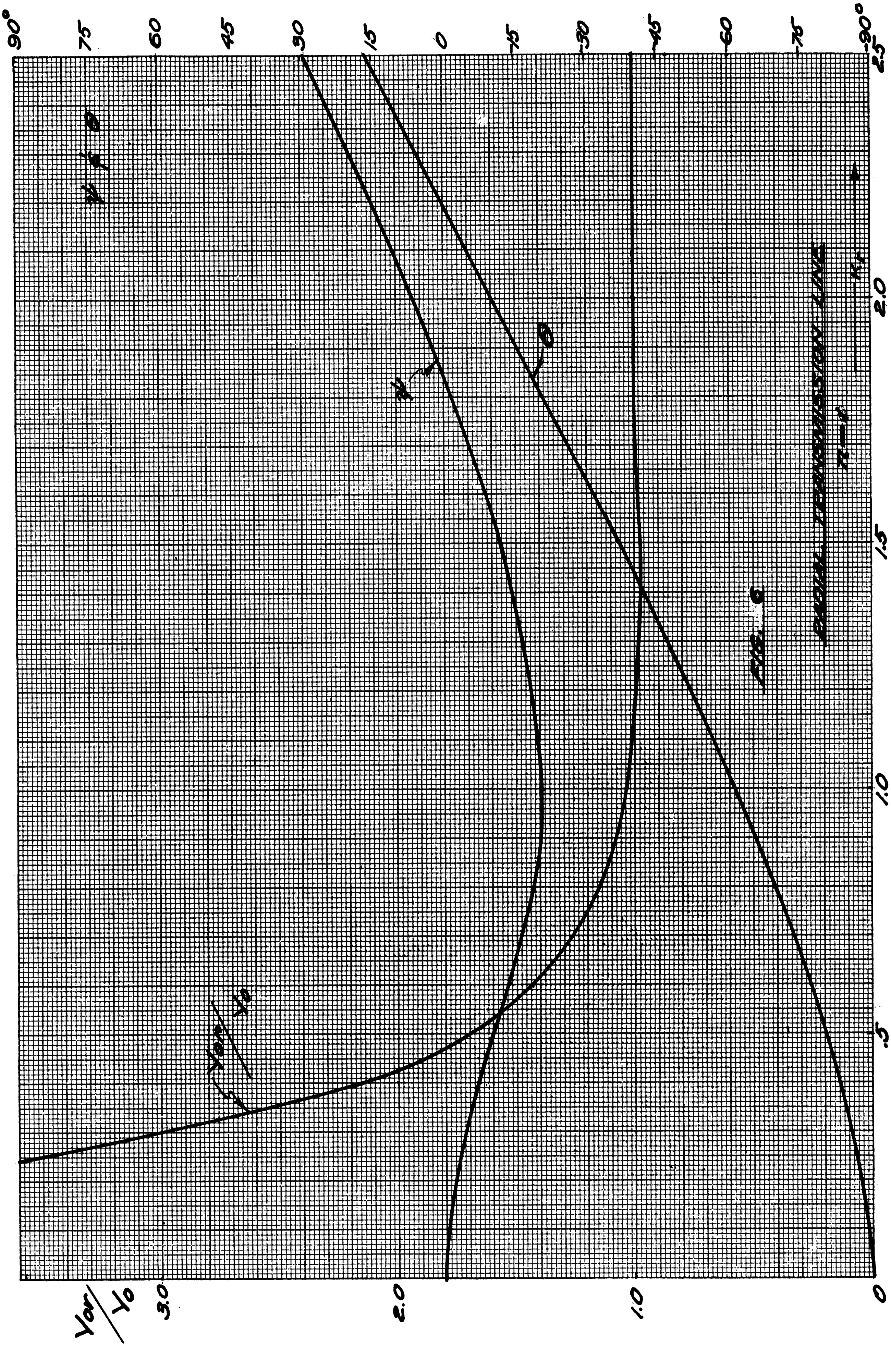

FIG. 6

RADIAL TRANSMISSION LINE

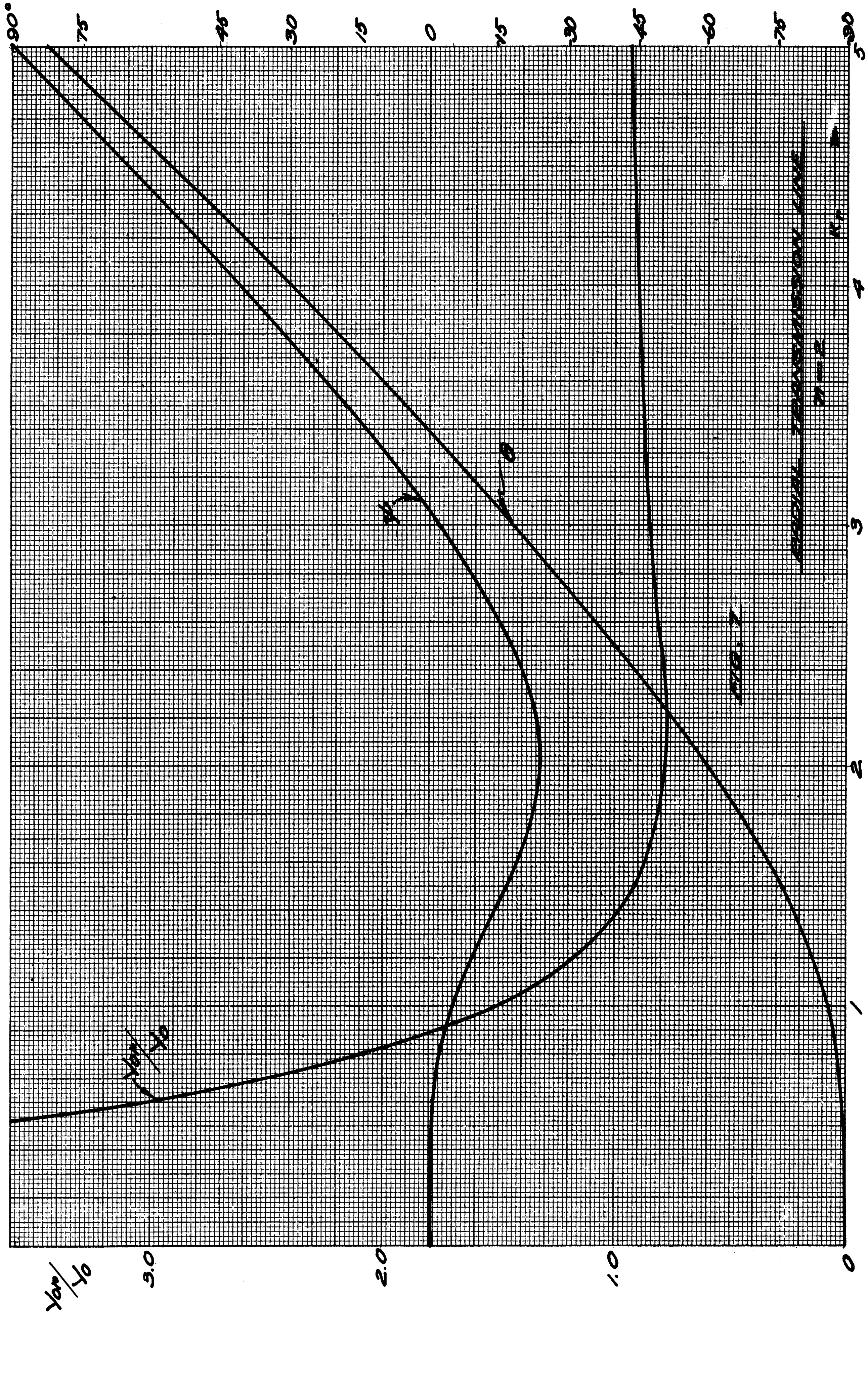

RADIAL TRANSMISSION LINE
n=2
kr
FIG. 7
θ
ψ
Y0n/Y0
90°
75
45
30
15
0
15
30
45
60
75
90
0
1
2
3
4
5
3.0
2.0
1.0
0

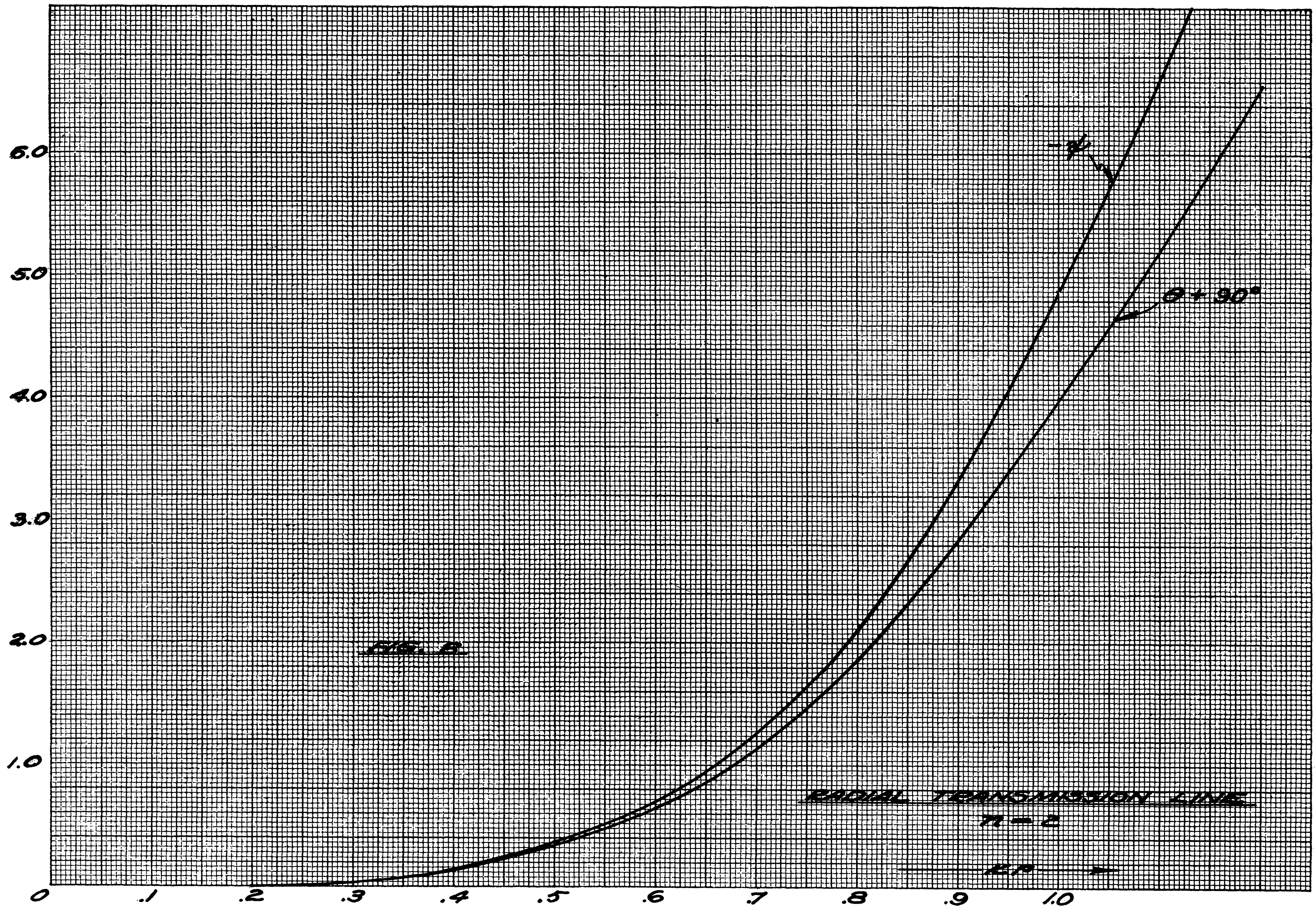
-ψ
θ + 90°
RADIAL TRANSMISSION LINE
n = 2
kρ
0
.1
.2
.3
.4
.5
.6
.7
.8
.9
1.0
2.0
3.0
4.0
5.0
6.0

FIG. 6

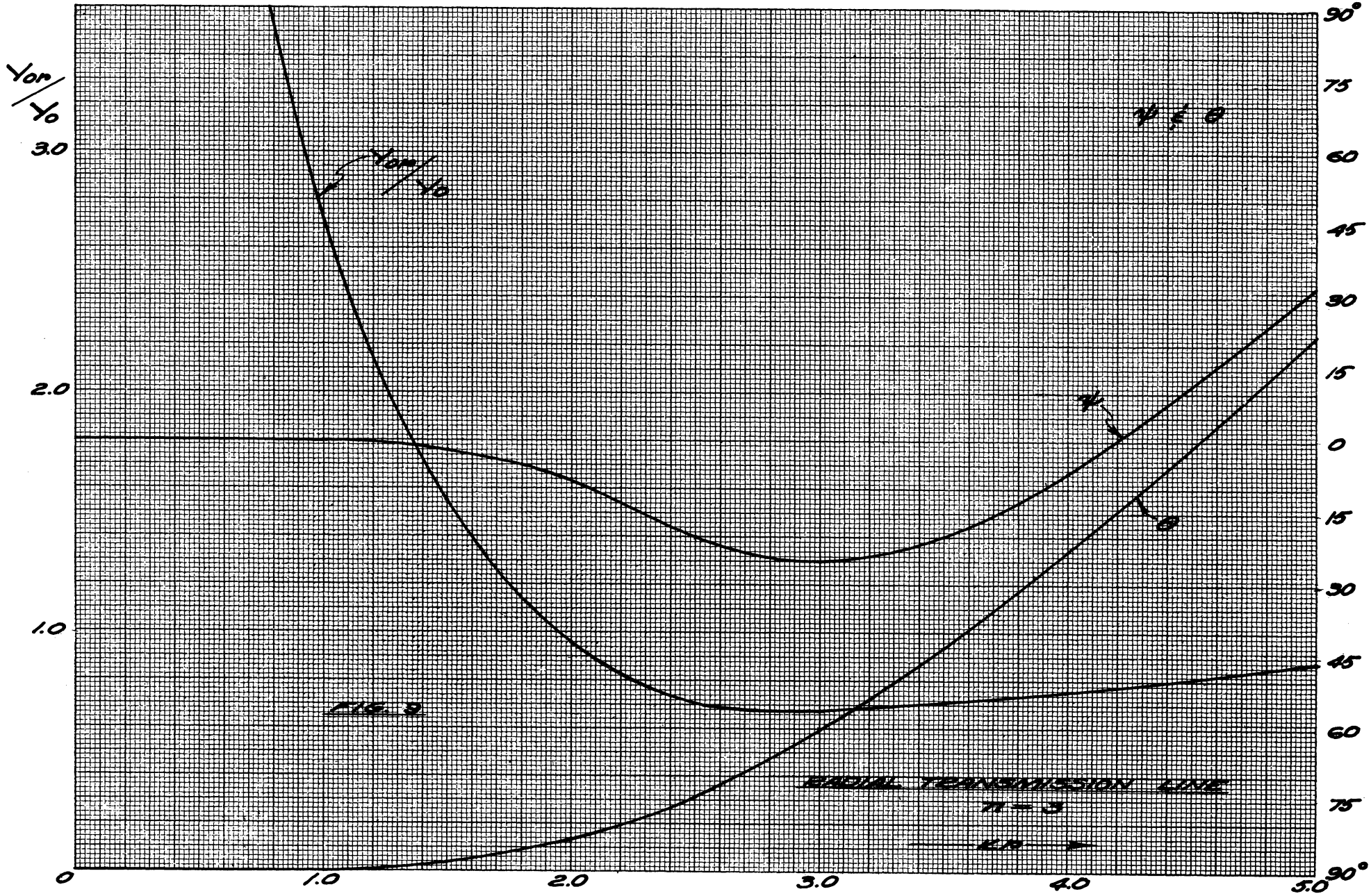
Y_{0r}/Y_0
3.0
2.0
1.0
0
1.0
2.0
3.0
4.0
5.0
90°
75
60
45
30
15
0
15
30
45
60
75
90°
Y_{0r}/Y_0
ψ & θ
ψ
θ
FIG. 2
RADIAL TRANSMISSION LINE
$n = 3$
$K_R =$

TE and TM waves in the central cavity as well as in the extension. A very rough approximation for $n > 0$ can be obtained by considering only the TM-wave represented by (20) in the central cavity and the lowest order TE-wave in each end space. The equivalent reactances of these three waves may all be regarded as lumped constants connected in series.

The equations (7) to (12) above give the general expressions for the TE-waves. In the same way as for the TM-waves we can introduce Hankel functions for $Z_n(kr)$.

$$Z'_n(k_r r) = j \bar{G}_n (-Ae^{j\psi} + Be^{-j\psi}) \quad . \tag{21}$$

After introduction of the boundary condition $E_\varphi = 0$ at $r = r_{al}$ this becomes

$$Z'_n(k_r r) = \bar{G}_n \sin(\psi_a - \psi) \quad . \tag{22}$$

To make $E_\varphi = 0$ also at $r = r_k$ we must have

$$\sin(\psi_a - \psi_k) = 0 \quad . \tag{23}$$

For the lowest-order mode then

$$\psi_a - \psi_k = 180^\circ \quad . \tag{24}$$

Because of the transcendental nature of these relations, a graphical solution is convenient (Fig. 10). The intersection between a curve of $k_r r_{al}$ vs. $k_r r_k$ obtained from (24) and a straight line through the origin with the slope r_a/r_k gives k_r. From (13)

$$k_y = k \sqrt{1 - (k_r/k)^2} \quad , \tag{25}$$

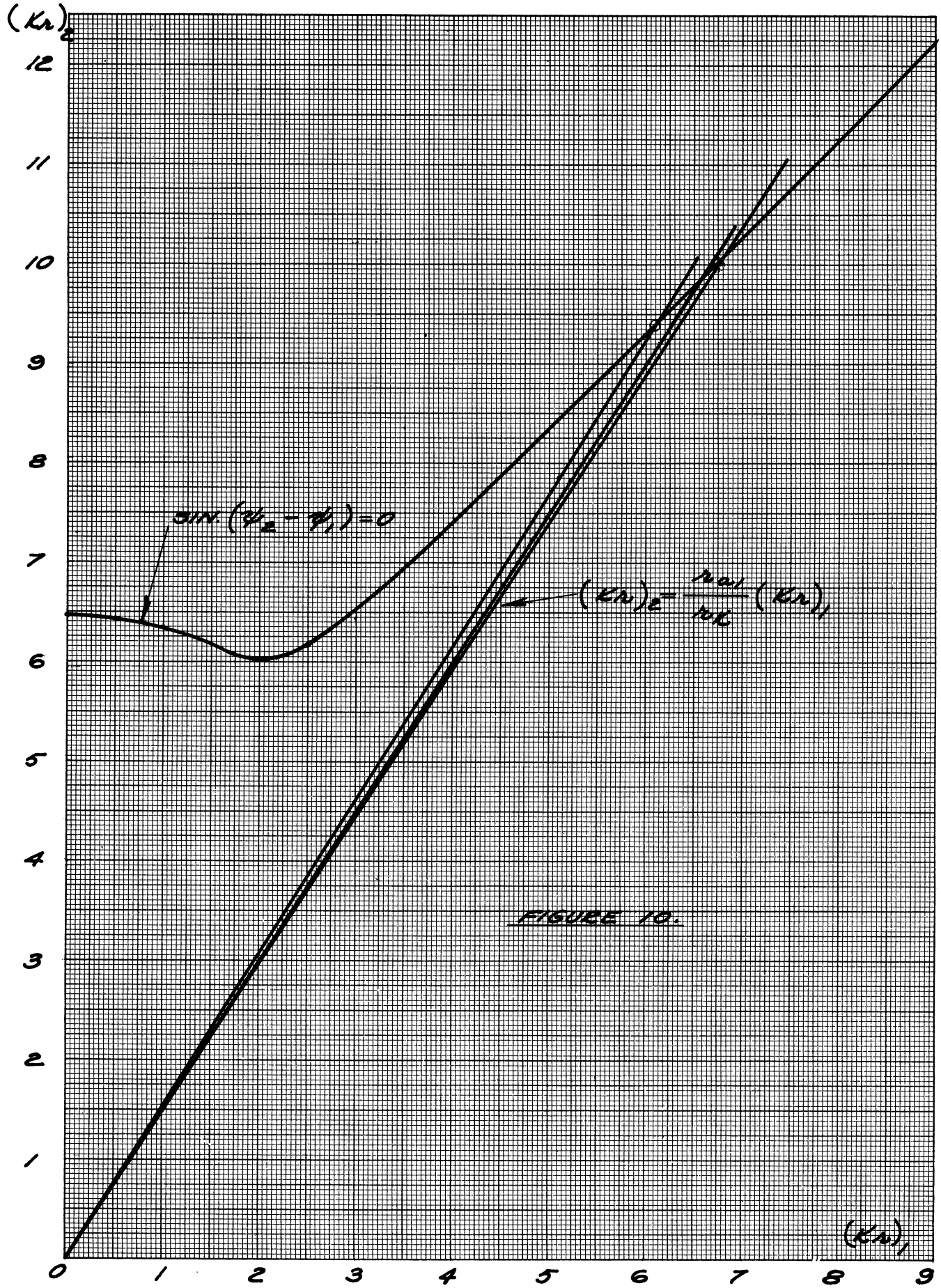
$(kr)_2$
12
11
10
9
8
7
6
5
4
3
2
1
0
1
2
3
4
5
6
7
8
9
$(kr)_1$
$\sin.(\psi_2 - \psi_1) = 0$
$(kr)_2 = \frac{r_2 a_1}{r_1 a_2}(kr)_1$

FIGURE 10.

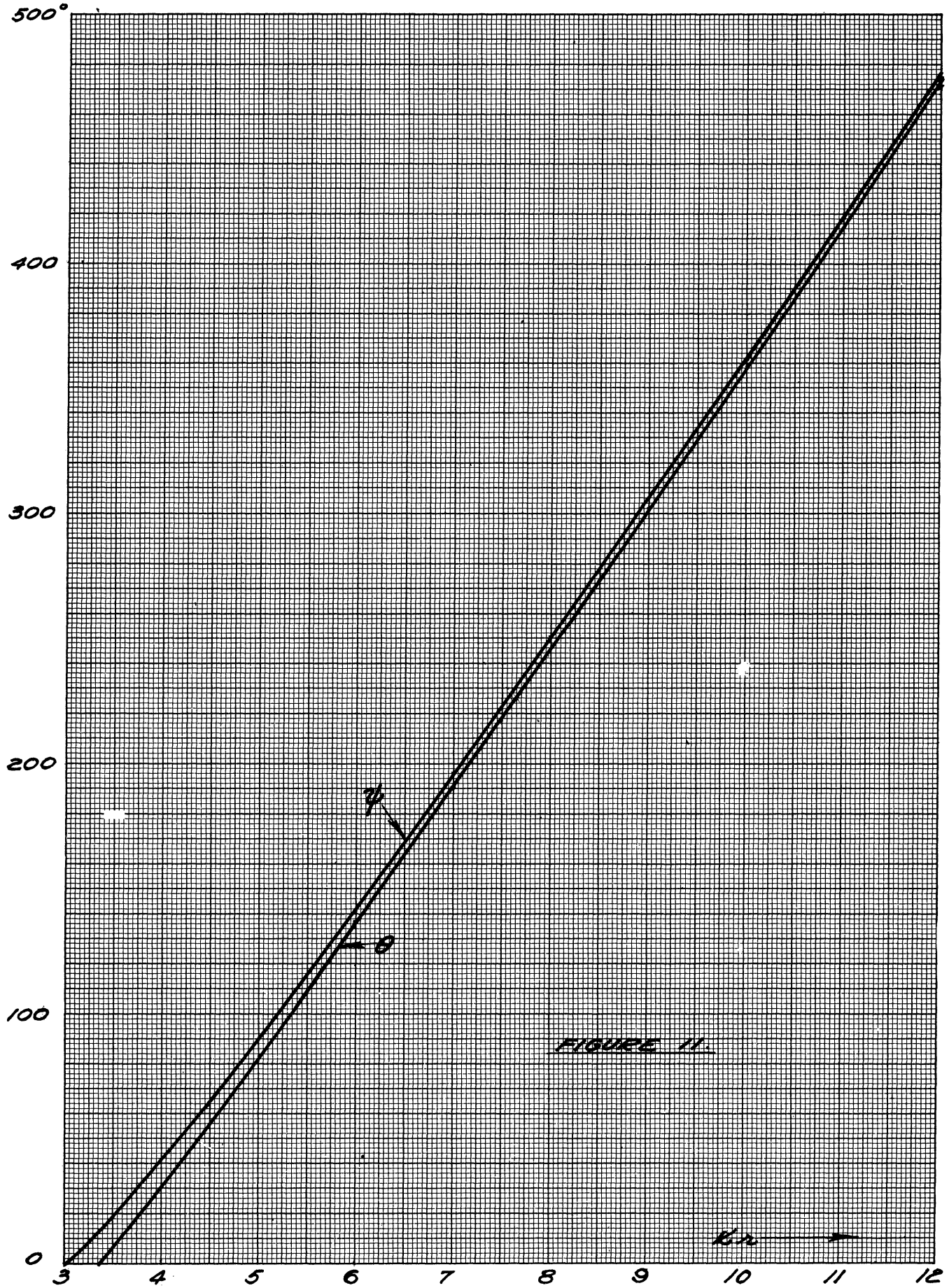

FIGURE 11.

which will in general be imaginary so that there is attenuation rather than propagation axially.

The wave admittance of one of the extensions then is

$$\bar{Y}_e = \frac{k_y}{k} \cdot Y_o \tag{26}$$

The total admittance of an end space is the total power flow divided by the mean square at a point of maximum voltage.

$$Y_e = \frac{\int_0^{2\pi} \int_{r_k}^{r_a} (\mathcal{E}_r H_\varphi + \mathcal{E}_\varphi H_r)\, r \cos n\varphi \, dr \, d\varphi}{\left\{ \int_{r_k}^{r_a} \mathcal{E}_r \, dr \right\}^2} . \tag{27}$$

For n = 2 this expression reduces to

$$Y_e = \frac{\pi . k_y . Y_o \left\{ Z_2^{\,2}(k_r r_k) \left[4 - (k_r r_k)^2 \right] - Z_2^{\,2}(k_r r_a) \left[4 - (k_1 r_a)^2 \right] \right\}^2}{32\, k \left\{ \frac{Z_2(k_r r_k)}{(k_r r_k)^2} - \frac{Z_2(k_r r_a)}{(k_r r_a)^2} \right\}} , \tag{28}$$

where $Z_2(kr) = G_2(kr) \cos(\theta - \psi_k)$ (Fig. 12).

The modified admittance of interaction space then is approximately

$$Y_{al}' = \frac{Y_{al} \cdot Y_e/2}{Y_a + Y_e/2} = \frac{Y_{al} \cdot Y_e}{2\, Y_{al} + Y_e} \tag{29}$$

$$Y_{al} = \frac{\pi r_{al}}{h} \cdot \bar{Y}_{al}$$

We have here assumed that the axial direction is sufficiently long and the attenuation constant jk_z sufficiently large so that the waves reflected from the ends are insignificant.

4. Finger System

The susceptance of the finger system depends on the properties of this configuration as a radial transmission line and on the boundary phenomena at r_{a1} and r_{a2}. The possibility of calculating this susceptance by harmonic analysis by evaluating the complete spectrum of modes in the three line sections has been investigated. Because of the unfavorable ratio of the effective cross section of the line sections - somewhat larger than 0.5 - the series of modes converges very slowly, so that this method is impractical. The success of the Harvard group in predicting the resonance frequencies from computations of the static capacitance of the finger system and a rather rough evaluation of the inductive susceptance has led the author to use their methods with minor revisions.

The static capacitance is

$$C_f = \epsilon_o N \left[h - 2g\right] \left\{\frac{t}{d} + \frac{1}{\pi}\left(\frac{d+w}{w}\log\frac{2d+w}{d} + \log\frac{w(2d+w)}{d^2}\right)\right.$$

$$\left. + \epsilon_o N w\left\{\frac{4}{\pi}\log\csc\frac{\pi g}{2h} + \frac{t}{g}\right\}\right. , \qquad (30)$$

where ϵ_o is the dielectric constant of free space and N is the total number of fingers. Other notation is presented in Fig. 2. For a mode number $n > 0$ the capacitance is 1/2 of this value.

This capacitance is derived for a uniform finger distribution (Fig. 2A). Since a finger system with phase reversals (Fig. 2B) differs from the former configuration only where the electric field is close to zero, the same formula can be used if N is interpreted as the equivalent rather than the actual number of fingers ($N = 2\pi r_{a1}/(d + w)$).

The inductive susceptance is assumed to be due to the radial component of the magnetic field between the fingers. This component is taken to be the average of the computed values of the radial component of the desired mode in the cylindrical sections at r_{a1} and r_{a2} multiplied by the ratio of the total volume between r_{a1} and r_{a2} and the net volume accessible to the magnetic field (i.e., the volume between the fingers). This quantity is squared and multiplied by $\mu_o/2$ times the net volume accessible to the magnetic field. The magnetic energy of the higher-order modes in the cylindrical sections is neglected.

If the axial electric field at r_{a1} and r_{a2} is $\mathcal{E}_a$, the reactive "power" in this susceptance can be expressed as ω times the stored energy or, alternatively, as one-half the volume integral of the square of of the electric field times an equivalent wave susceptance - $\bar{B}_{fm}$ as follows:

$$\frac{\omega\mu_o}{4}\left[\left(\frac{1}{r_{a1}}+\frac{1}{r_{a2}}\right)\frac{n}{2k}\,Y_o\,\mathcal{E}_a\,\frac{V}{V_a}\right]^2\cdot V_a \;=\; \frac{1}{4}\,\mathcal{E}_a^{\,2}(-\bar{B}_{fm})\,2\pi r_{a2}h \qquad (31)$$

$$\text{or} \qquad -\bar{B}_{fm} \;=\; \omega\mu_o\left[\left(\frac{1}{r_{a1}}+\frac{1}{r_{a2}}\right)\frac{n}{2k}\cdot Y_o\,\frac{V}{V_a}\right]^2\;\frac{V_a}{2\pi r_{a2}\cdot h}\cdot \qquad (32)$$

Here V is the total volume between the surfaces of radii r_{a1} and r_{a2} and V_a is the part of this volume that is not filled with copper.

In order to account for the influence of the end spaces, the term $1/r_{a1}$ within the brackets above should be reduced in the ratio $Y_e/(Y_e + 2Y_a)$ or Y'_a/Y_a.

5. Resonance Equation

The resonance criterion can be stated in the following form for the Model A geometry:

$$\frac{\omega C_f}{2}\cdot\frac{h}{\pi r_{a2}} + \bar{B}_{fm} - y_{oa2}\cdot Y_o \frac{\cos(\theta_b - \psi_{a2})}{\sin(\theta_b - \theta_{a2})} - \frac{r_{a1}}{r_{a2}} y_{oa1} Y_o \frac{\cos(\psi_{a1} - \theta_k)}{\sin(\theta_{a1} - \theta_k)} = 0 , \tag{33}$$

where C_f and $\bar{B}_{fm}$ are given by (30) and (32).

In design problems the resonance frequency is given and some of the geometrical parameters are left to be determined. Except in the slowly varying term containing log csc $\frac{\pi g}{2h}$ in (30) the axial height h and the radial thickness t of the fingers appear in an algebraically simple way in (33), so that either of these dimensions can easily be adjusted so that (33) is satisfied for the desired frequency.

6. Energy Storage

If the four susceptances included in the left member of (33) were each a pure inductive or a pure capacitive susceptance, respectively, the evaluation of the energy storage in the resonator would be extremely simple. However, only the first two terms are "pure" in this sense; the cavity sections inside and outside the finger system although predominantly inductive do hold also some electric energy storage.

The stored electric energy and magnetic energies, respectively, are:

$$W_E = \frac{\epsilon_o}{2}\int_V \mathcal{E}^2 dV = \frac{\epsilon_o}{2}\int_V \mathcal{E}_z^2\, dV \tag{34}$$

$$W_H = \frac{\mu_o}{2}\int_V \mathcal{H}^2\, dV = \frac{\mu_o}{2}\int_V (\mathcal{H}_r^2 + \mathcal{H}_\varphi^2) dV \tag{35}$$

If these integrations are carried out and the result expressed in terms of the quantities G_n, $\bar{G}_n$, θ and ψ previously defined, we get for the space between r_k and r_a,

$$W_{E1} = \frac{\epsilon_o}{4}\pi h \mathcal{E}_a^2 \left\{ r_{al}^2 \left[1 - \left(\frac{n}{kr_{al}}\right)^2 + b_{al}^2 \right] - r_k^2 \left[\frac{\bar{G}_n(kr_k)\cos(\psi_k - \theta_k)}{G_n(kr_{al})\sin(\theta - \beta_h)} \right]^2 \right\} \tag{36}$$

$$W_{H1} = \frac{\mu_o}{4}\pi h \mathcal{E}_a^2 Y_o^2 \left\{ r_{al}^2 \left[1 - \left(\frac{n}{kr_{al}}\right)^2 + \frac{2b_{al}}{kr_{al}} + b_{al}^2 \right] \right.$$

$$\left. - \left[\frac{\bar{G}_n(kr_k)\cos(\psi_k - \theta_k)}{G_n(kr_{al})\sin(\theta_{al} - \theta_k)} \right]^2 \right\} . \tag{37}$$

Here

$$b_{al} = - \frac{\bar{G}_n(kr_{al})\cos(\psi_{al} - \theta_k)}{G_n)kr_{al})\sin(\theta_{al} - \theta_k)} . \tag{38}$$

The coefficients in front of the brackets in (36) and (37) are identical, since

$$Y_o = \sqrt{\epsilon_o/\mu_o} . \tag{39}$$

Consequently

$$W_{H1} - W_{E1} = \frac{\epsilon_o}{4} \pi h \zeta_a^2 r_{a1}^2 \frac{2b_{a1}}{kh_{a1}} = \frac{1}{4\omega} 2\pi r_{a1} h \bar{B}_{a1} \zeta_a^2 \quad . \tag{40}$$

The difference between the magnetic and electric energy is equal to the energy stored in a pure inductive susceptance of the same magnitude as the actual susceptance. Equation (40) shows that (36), (37) and (20) are consistent with this statement.

Analogous expressions are obtained for the stored energy in the cavity external to the finger system. The short-circuited end of the radial transmission line will be the upper limit of integration so that the two terms inside brackets are interchanged, as the subscripts k are changed to b. Since we are now measuring the susceptance looking towards positive instead of negative r the magnetic field and the susceptance have to be taken with reversed sign. This reversal is cancelled, however, if the sine function in the denominator is written sin $(\theta_b - \theta_{a2})$.

In (36) and (37) the amplitude functions G_n and $\bar{G}_n$ appear separately; since we have so far given curves only for their ratio y_{or} (Figs. 5-9) G_n and $\bar{G}_n$ are plotted in Figs. 12, 13 and 14 for n = 2.

Since the input conductance at the anode is specified we can now predict the Q of the resonator. From the stored energy we can calculate an "equivalent susceptance" B_e at r_{a2} $(n > o)$

$$\omega W_E = \frac{1}{4} \zeta_a^2 . B_E 2\pi r_{a2} . h \quad . \tag{41}$$

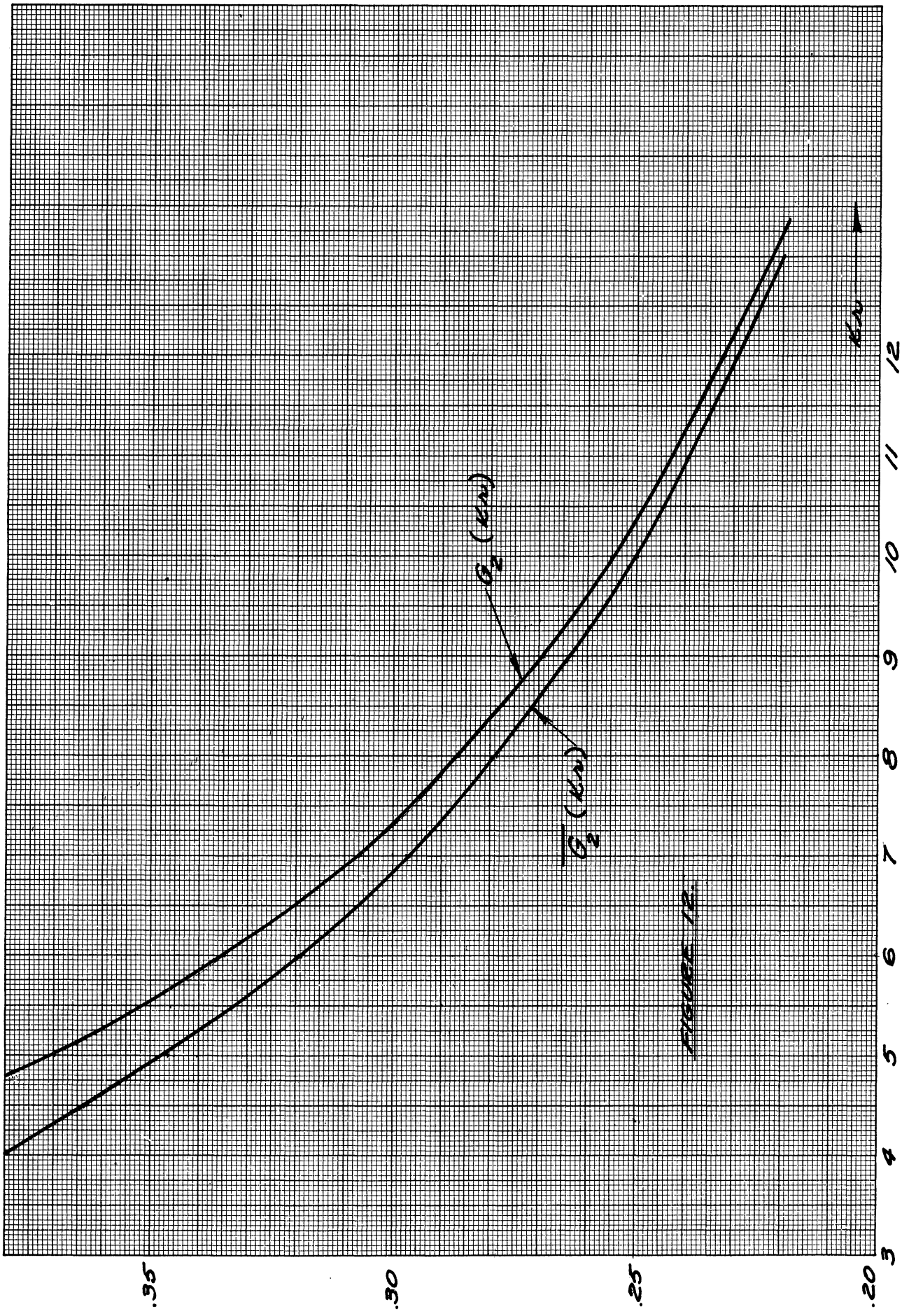

FIGURE 12.

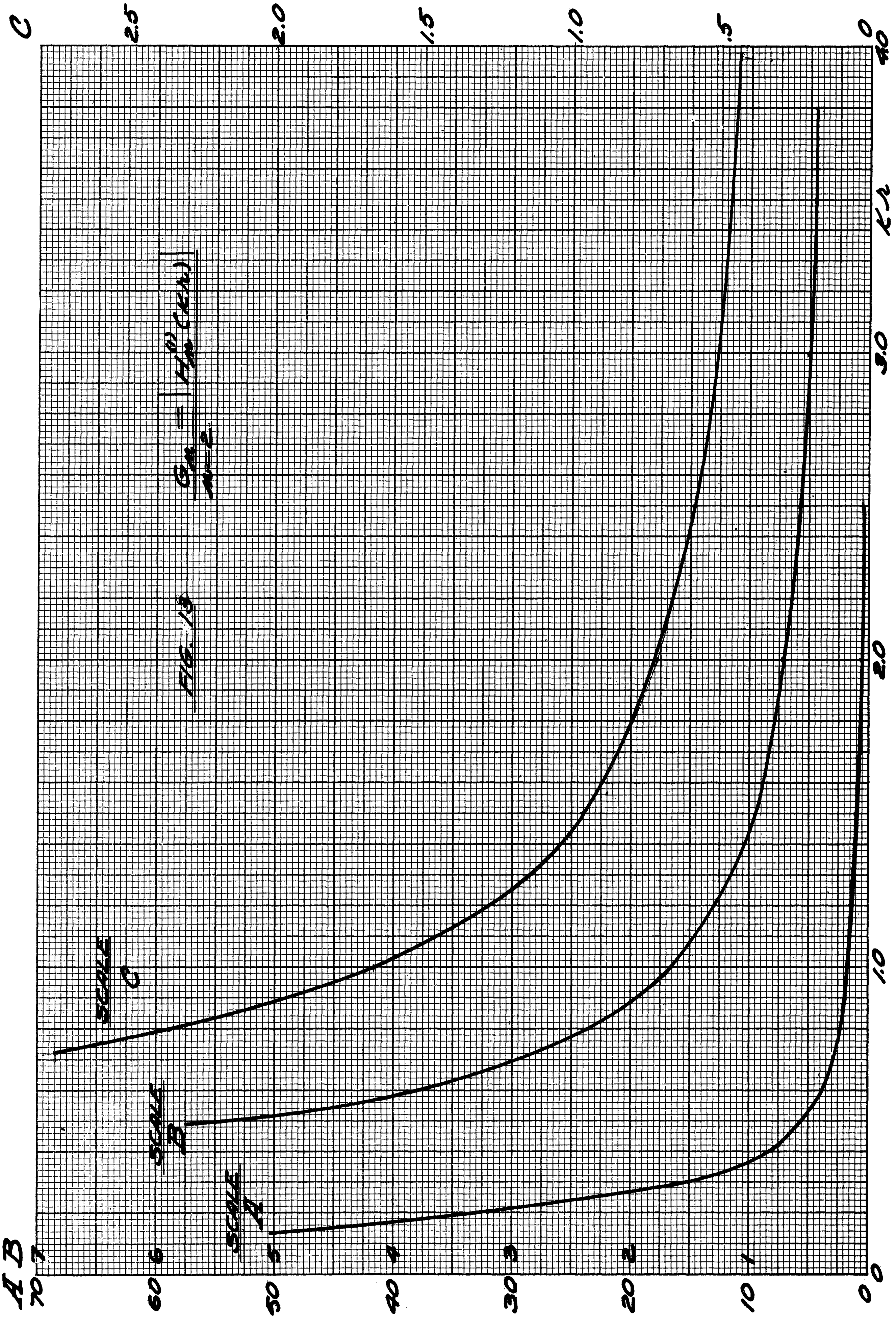
FIG. 15
$G_m = |H_m^{(1)}(kr)|$, $m=2$
SCALE A
SCALE B
SCALE C
A B C
kr
0 1.0 2.0 3.0 4.0
0 .5 1.0 1.5 2.0 2.5
0 10 20 30 40 50 60 70
0 1 2 3 4 5 6 7

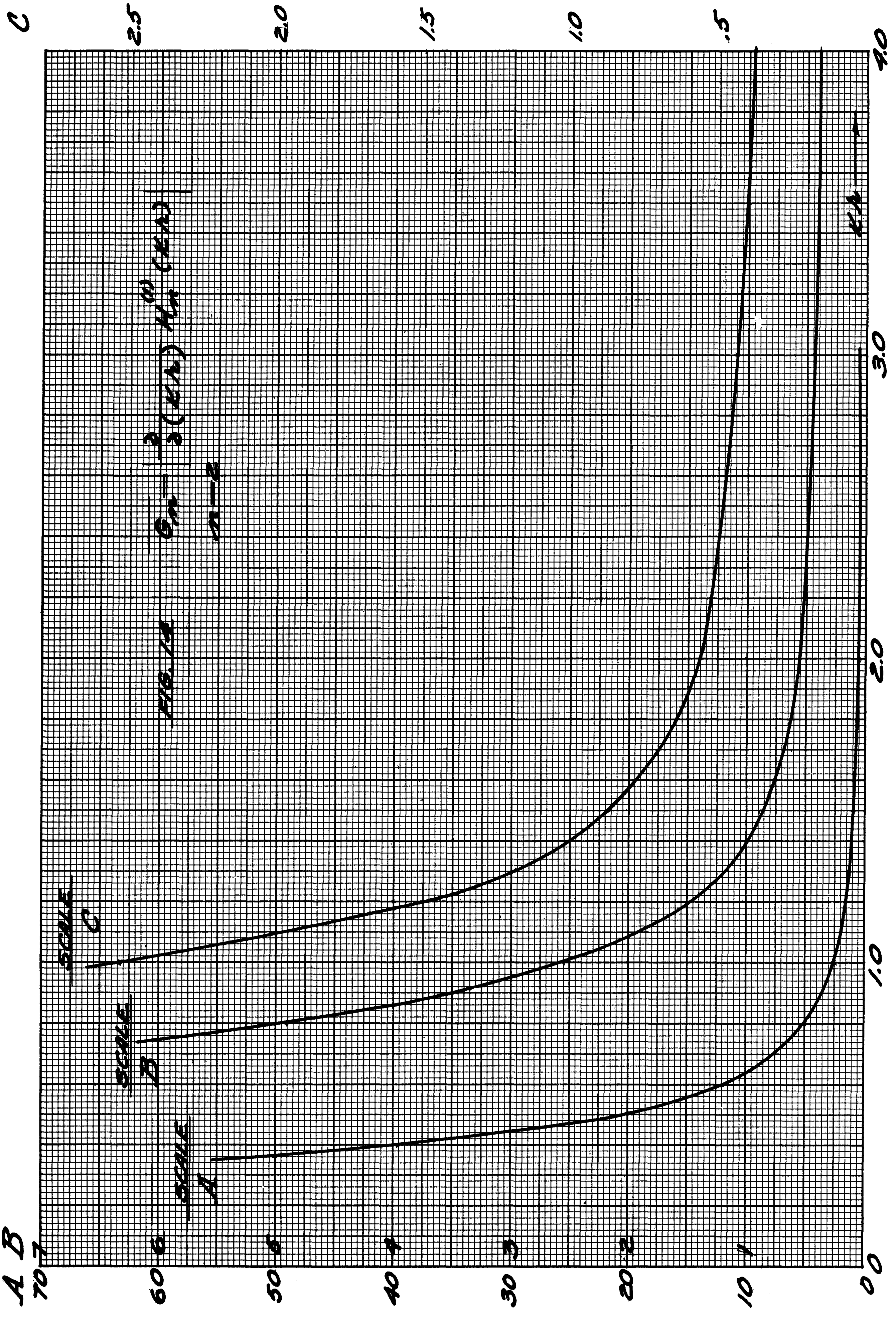
FIG. 14
$G_n = \left| \frac{\partial}{\partial (ka)} H_n^{(1)}(ka) \right|$
n = 2
SCALE A
SCALE B
SCALE C
ka
A B C
0 0 1.0 2.0 3.0 4.0
70 7 60 6 50 5 40 4 30 3 20 2 10 1 0 0
.5 1.0 1.5 2.0 2.5

Then

$$Q_L = \frac{\bar{B}_E}{\bar{G}_{a2}} \quad , \tag{42}$$

where $\bar{B}_E$ is the equivalent capacitive wave susceptance at $r = r_{a2}$ and $\bar{G}_{a2}$ is the wave conductance consistent with the specified electronic input conductance. (See page 20)

The representation of the energy storage by an equivalent capacitance makes it unnecessary to make correction for the end spaces, since the electrical energy storage there is a second-order small quantity compared to the total energy storage.

The skin resistance of a unit area is

$$R_s = \sqrt{\frac{\omega\mu}{2\sigma}} \quad . \tag{43}$$

where μ and σ are the permeability and the conductivity, respectively, of the conductor.

The current per unit length is perpendicular to and (in the mks system) numerically equal to the tangential magnetic field at the surface of the conductor. The loss in the space inside the finger system then is

$$P_{d1} = \frac{R_s}{2}\left\{\pi r_k h \cdot H_\varphi^2(r_k) + 2\int_{r_k}^{r_{a1}} \pi r\left(H_r^2 + H_\varphi^2\right) dr\right.$$

$$= \frac{R_a}{2}\pi \cdot \mathcal{E}_a^2 \cdot Y_o^2 \left\{ r_{a1}^2 \left[1 - \left(\frac{n}{kr_{a1}}\right)^2 - \frac{2b_{a1}}{kr_{a1}} + b_{a1}^2\right]\right. \tag{44}$$

$$\left. + r_k(h - r_k)\left[\frac{\bar{G}_n(kr_k)\cos(\psi_k - \theta_k)}{G_n(kr_{a1})\sin(\theta_{a1} - \theta_k)}\right]^2 \right\} \quad .$$

It is interesting to note that when the axial height is equal to the cathode radius r_k the only term in (35) that depends on r_k and h disappears. This means that the actual loss in the cathode surface is equal to the additional loss that would have occurred in the end walls if there had been no cathode.

Similarly the loss in the cavity external to the finger system is

$$P_{d2} = \frac{R_s}{2} \pi \mathcal{E}_a^2 . Y_o^2 \left\{ r_b(r_b + h) \left[\frac{\bar{G}_n(kr_b) \cos(\theta_b - \psi_b)}{G_n(kr_{a2}) \sin(\theta_b - \theta_{a2})} \right]^2 - \right.$$

$$\left. - r_{a2}^2 \left[1 - \left(\frac{n}{kr_{a2}}\right)^2 + \frac{2b_{a2}}{kr_{a2}} + b_{a2}^2 \right] \right\} \quad . \tag{45}$$

The copper losses in the fingers should similarly be calculated from the radial and axial magnetic field components tangential to the finger surfaces. To know these components exactly we should have to determine the complete mode spectrum required to satisfy the boundary conditions at the finger surfaces. It appears that the predominant high-order modes produced by reflection from the fingers have large wave admittances. A minimum value of the tangential magnetic field would consequently be twice the field calculated from the main mode in the cylindrical cavity, with a probable value appreciable higher than that. As an approximate value we can write

$$P_{df} = \frac{R_s}{2} \pi (\mathcal{E}_a Y_o)^2 \left\{ \frac{Nt}{\pi} (2h - 2g + d + w) \left[\frac{n}{2} \left(\frac{1}{kr_{a1}} + \frac{1}{kr_{a2}} \right) \frac{V}{V_a} \right]^2 + \right.$$

$$\left. + 4(h - g) \left[r_{a1} (b_{a1})^2 + r_{a2} (b_{a2})^2 \right] \right\} \quad . \tag{46}$$

The total copper loss in the resonator $P_d = P_{d_1} + P_{d_2} + P_{d_f}$ produces an equivalent conductance at $r = r_{a2}$

$$\bar{G}_d = \frac{P_d}{\pi r_{a2} h \mathcal{E}_a^2} \quad . \tag{47}$$

All the expressions for the losses given above contain the factor $\mathcal{E}_a^2$, which consequently cancels out in (47), so that $\bar{G}_d$ is obtained in terms of R_s, Y_o, λ, and the geometry parameters only.

(47) determines the internal Q of the resonator, since

$$Q_o = \frac{\bar{B}_E}{\bar{G}_d} \quad . \tag{48}$$

and the circuit efficiency

$$\eta_c = \frac{\bar{G}_{a2} - \bar{G}_d}{\bar{G}_{a2}} \quad . \tag{49}$$

B. DESIGN PROCEDURE

The objective of design as far as impedance transformation is concerned is to ascertain that the conductance between the anode segments, the slot conductance, is close to the optimum for the electronic operation and that as large a fraction as possible of the power generated by the electronic system is delivered to the output wave guide.

The optimum slot conductance is conveniently given for an ideal π-mode, that is for π radians phase difference between the r-f voltages across consecutive slots and equal voltage magnitude across all slots. In those interdigital magnetrons where $n > 0$ in (1), the slot voltage varies from a maximum value E_a at certain slots to zero

at other slots. A Fourier expansion of this slot voltage gives an equivalent π-mode voltage

$$E_\pi \cong \frac{1}{2} \mathcal{E}_a . h \tag{69}$$

where $\mathcal{E}_a$ as before is the axial electric field strength. The potential difference between adjacent fingers is assumed to be constant along the entire length of the fingers. Equation (69) concerns a uniform arrangement of the fingers (Fig. 2A). If the phase reversals at the nodes are introduced (Fig. 2B) and the tube is operated with the value of n for which it is designed

$$E_\pi \cong \frac{2}{\pi} \mathcal{E}_a . h \tag{70}$$

The π-mode slot conductance G_π is obtained by setting the power delivered by the electrons equal to the power transmitted by the cavity. We assume that only the π-component of the slot voltage exchanges any appreciable power with the electrons in the interaction space

$$\frac{1}{2} E_\pi^{\,2} G_\pi = \frac{1}{2} \bar{G}_a r_{a2} h \int_0^{2\pi} (\mathcal{E}_a \sin n\varphi)^2 \, d\varphi \ . \tag{71}$$

Introducing (70) into (71), we obtain

$$\bar{G}_a \cong \frac{4h}{\pi^2 r_{a2}} G_\pi \ . \tag{72}$$

In order to realize this wave conductance $\bar{G}_a$, the impedance transformation from the wave guide to the anode segments should produce a wave-conductance component at the anode equal to:

$$\bar{G}_a' = \bar{G}_a - \bar{G}_d \tag{73}$$

where $\bar{G}_d$ is the loss conductance given by (47). Under such conditions the circuit efficiency of the resonator becomes

$$\eta_c = \frac{\bar{G}_a - \bar{G}_d}{\bar{G}_a} \tag{49}$$

If this figure proves to be too low, it is necessary either to redesign the electronic system so that a larger value of $\bar{G}_a$ can be permitted or to reduce the loss conductance of the resonator. The largest part of the copper losses occurs in the fingers; a reduction of the area of the fingers should consequently reduce the losses. At the same time, however, the cooling of the fingers becomes poorer. A lower value of the azimuthal mode number n gives lower magnetic field strength at the fingers, but for the same resonance frequency the geometrical dimensions become smaller.

At this point the energy storage and Q should be checked to make sure that reasonable frequency stability will be obtained [(36), (41) and (42)].

The real part of (18) gives a relation between $\bar{G}_{a2}$ and the loading ratio η_b at the circumference of the cavity. If η_b is assumed to be a real number, we obtain:

$$G_a' = y_{oa2}\, Y_o \frac{\eta_b \{\cos(\theta_b - \psi_{a2}) \cos(\psi_b - \theta_{a2}) + \sin(\psi_b - \psi_{a2}) \sin(\theta_b - \theta_{a2})\}}{\cos^2(\psi_b - \theta_{a2}) + \eta_b^2 \sin^2(\theta_b - \theta_{a2})} \tag{74}$$

Since the Q of the resonator is of the order of 100, η_b will be a large quantity, so that the first term in the denominator can be neglected

in comparison with the second, and η_b is very simply obtained from (36). The wave conductance at the edge of the cavity is then

$$\bar{G}_b = \eta_b y_{ob} Y_o \quad . \tag{75}$$

The transformer section should now be so designed that the wave conductance produced at the boundary r_b has this value.

The characteristic wave admittance of the output wave guide is

$$\bar{Y}_{og} = Y_o \sqrt{1 - (\lambda/4b_g)^2} \quad . \tag{76}$$

where $2b_g$ is the width of the wave guide.

The first approximation of the admittance seen from the transformer when the wave guide is terminated in its characteristic admittance is, from (13) in Part I of this paper,

$$\bar{Y}_{T_t} \approx \alpha_{t_g}^2 \bar{Y}_{og} \quad . \tag{77}$$

The characteristic wave admittance of the transformer section is

$$\bar{Y}_{ot} = Y_o \sqrt{1 - (\lambda/4b_t)^2} \quad . \tag{78}$$

where $2b_t$ is the width of the transformer section.

The wave admittance at the transformer side of the boundary r_b

$$\bar{Y}_{Tb} \approx \frac{\bar{Y}_{ot}^2}{\bar{Y}_{og} \alpha_{tg}^2} \quad . \tag{79}$$

We have here assumed that the length of the transformer section is made exactly a quarter of the guide wavelength. If this is not the case, (19) should be used for the step from (77) to a more complete form of (79).

If the curvature of the boundary surface at $r = r_b$ is disregarded the first approximation of the wave admittance on the cavity side of the boundary is

$$\bar{Y}_b \cong \bar{G}_b \cong \frac{Y_{ot}^2}{Y_{og} \cdot \alpha_{tg}^2 \cdot \alpha_{tc}^2} \tag{80}$$

Since all the modes involved here have no variation in the y-direction

$$\alpha_{tg}^2 = \frac{t}{h_g} \cdot \beta_{tg}^2 \tag{81}$$

$$\alpha_{tc}^2 = \frac{t}{h_c} \cdot \beta_{tc}^2 \tag{82}$$

where $2h_g$, $2t$, and $2h_c$ are the heights of the wave guide, transformer, and cavity, respectively, and β_{bg}, β_{tc} are constants determined by the width of these units according to relations corresponding to (23) to (28) in the first part of this paper. In (80) t^2 thus appears in the denominator of the right member, and the value of t can be so chosen that $\bar{G}_b$ gets the desired value computed in (75).

The facts that no allowance has been made for the transformation from cylindrical to plane waves and that the shunt susceptances at the junctions have been neglected may introduce an appreciable error in the results obtained by this procedure. The numerical calculations and the model tests reported in the next section show that the external

Q is likely to be 50 to 100% larger than the design value chosen by the approximate procedure above. A check based on the results in Section B of Part I is therefore desirable.

First a closer approximation of the wave admittance at the output end of the transformer is obtained by adding in (77) a susceptance component. This susceptance is most conveniently determined from graphs and formulas available in the literature.

The next step is to compute the reflection coefficient corresponding to this termination and referred to the origin ($z = 0$). This quantity is introduced in (79) and (80) in Part I, and the coefficients a_{v1} and b_{v1} are calculated for r_c equal to the radius of the cylindrical surface terminating the straight part of the transformer section. Equation (73), Part I, then gives the admittance to the principal cylindrical wave at this surface. The admittance on the transformer side of the junction between cavity and transformer can next be calculated by application of (18), Part II. Dividing this admittance by the square of the proper coefficient of coupling η_{21} we obtain the terminating admittance $\bar{Y}_b$ of the cylindrical cavity and normalize it to η_b which now is a complex quantity. In order to obtain $\bar{G}'_{a2}$ with reasonable accuracy from (18), Part II, we write the real component of (18) in the following form

$$\bar{G}'_{a2} \cong y_{oa2}\, Y_o \frac{\left\{ \dfrac{\sin(\psi_b - \psi_{a2})}{\cos(\theta_b - \psi_{a2})} + \dfrac{\cos(\psi_b - \theta_{a2})}{\sin(\theta_b - \theta_{a2})} \right\} \rho}{\left\{ 1 + \dfrac{\cos(\psi_b - \theta_{a2})}{\sin(\theta_b - \theta_{a2})} \xi \right\}^2} ,$$

where

$$\rho + j\xi = \frac{1}{\eta_b}$$

$\bar{G}'_{a2}$ is roughly proportional to t^2, the square of the height of the transformer section. By comparing the value of $\bar{G}'_{a2}$ we just calculated with the desired value we can easily see how to adjust t so as to eliminate the difference.

It may seem inconsistent that the junction susceptance is accounted for on the output side of the transformer section but neglected on the input side. The reason is, of course, that the input admittance of the transformer is so large that the shunt susceptance at this point is relatively unimportant, even if it is not negligible.

The determination of the appropriate height of the transformer section completes the design computations. We shall in the next section compare calculations according to the analysis presented here with measurements on test models.

C. MODEL TESTS

In order to check the calculation procedure presented above a model cavity of the design and dimensions shown in Fig. 1 was subjected to a series of measurements. The cavity was designed to operate in the second-order mode ($n = 2$). The transformer section was so made that its length could be varied in three steps. Due to an error in the original calculations the height of the transformer was made too small, so that the external Q was very unrealistic and the circuit efficiency extremely poor. For the purpose of comparing measured and calculated data, however, this is unimportant. Before the tests were concluded, the transformer section was redesigned, so that a more realistic result was obtained in the last measurements.

Table I shows corresponding measured and calculated data for the test models. The column marked $1/2\,\epsilon_B$ indicates the error in resonance frequency. Because of the transcendental nature of the resonance equation the following indirect method was used to obtain this figure. At the measured resonance frequency the sum of the inductive susceptance and the sum of the capacitive susceptance at the radius of the finger system were calculated. Half the difference between these two sums in per cent is very nearly equal to the difference in per cent between the measured frequency and the frequency that satisfies the resonance equation with the calculated susceptances.

In the Q-measurements the standing-wave ratio was measured to 0.5 db or 15 % accuracy. Since in each case a curve of standing-wave ratio vs. wave length was plotted, the Q-values obtained from the measurements are probably somewhat more accurate than this figure indicates.

The computational errors may amount to a few per cent, since a slide rule was used throughout, and the calculations were rather lengthy, involving rationalization of complex fractions, etc.

The largest discrepancy between the measured and computed values is about 15 %. The maximum error in the calculations consequently is $\pm$ 30 % and the probable error considerably smaller than that, which is the best confirmation obtainable with the instrumentation employed.

It is interesting to compare the numerical results obtained in the first approximation (80), where the change from cylindrical to plane waves was disregarded, with those obtained in the final calcu-

lations, where an analytical transformation from plane to cylindrical waves was performed. The first-mentioned procedure gave the following values of Q_E in the same order as given in Table I, 1780, 1830, and 190, or not much more than half of the observed values. At the point in the transformer section where this transformation was introduced, the wave admittance in one case (Model B, 2t = .254cm) was $(1.47 + 2.61_j)Y_o$ according to the plane-wave approximation and $(3.09 + 4.43_j)Y_o$ according to the cylindrical-wave analysis. At the input end of the transformer section the corresponding figures were $(5.22 - 3.24_j)Y_o$ and $(2.53 - 4.49_j)Y_o$. The same terminating admittance was used in both calculations. In the transformation formula (73), Part I, six terms were included in numerator and denominator, accounting for cylinder waves of order zero to five. The highest-order terms included were small but not negligible.

The computation procedure given in this paper involves a number of approximations and simplifications that should be recapitulated and discussed at this point.

The general method of neglecting the resistivity of copper in the calculation of electromagnetic field configuration in resonators and wave guides has proved itself through the years and needs no justification. The influence of the higher-order modes generated in the transformer section by the discontinuities is very small. The cavity modes are not so easily dismissed. In the last model test (Model B, 2t = .81cm) the terminating admittance ratio in the cavity is $\eta_b = 23.2 - 11.4_j$, which is large enough to make non-resonant modes unimportant, but Q_E is still abnormally high and the circuit efficiency abnormally low. If Q_E were reduced to 100 or lower it would probably be

necessary to take the junction shunt susceptance into account. It should be noted that the terminating admittance has an appreciable susceptance component and that Q_E is more strongly dependent on the resistance than on the conductance of the cavity termination. Even a moderate change in the susceptance will produce a noticeable change in Q_E.

The most radical approximations concern the energy storage and copper loss in and in the immediate vicinity of the finger system. We must assume that the very good agreement in resonance frequency between calculations and observations is fortuitous.

In order to check how critical the length of the transformer section is, three different lengths were used with the observed results in Table II. The answer is evidently that Q_E remains substantially constant over a considerable range of transformer lengths. Incidentally, since the internal Q is independent of the output coupling, the table gives some indication of the random error in the measurements. The maximum deviation from the mean of Q_o is 6.9 % for Model A and 5% for Model B.

The numerical calculations for a second-order-mode resonator give some interesting information about energy distribution and losses in the resonator. It is not unexpected, of course, that about ninety per cent of the electric energy storage takes place in the immediate vicinity of the finger system. More remarkable is that the magnetic energy storage is about twice as large in interaction space as in the cavity external to the finger system. The finger system itself and the higher-order-modes in its vicinity account for twenty-five to thirty percent of the magnetic energy storage. About sixty to seventy per-

cent of the copper losses occur in the fingers, because these are immersed in the r-f magnetic field in a region of the resonator where both the radial and azimuthal components have their maximum values. If the same resistivity is assumed, the cathode surface accounts for another fifteen to twenty percent. Since the losses increase with the square root of the resistivity, this item may in an actual tube become an appreciable part of the total since the cathode surface has appreciably lower conductivity than copper. At room temperature tungsten and molybdenum would give more than twice the loss of copper, and at normal operating temperature considerably more. The loss in the cavity external to the finger system was found to be ten percent or less of the total. The losses in the end walls or the interaction-space extensions were found to be small compared to those previously mentioned.

TABLE I

		Observed Data			Calculated		
Test Cavity	Transformer Height	λ_o	Q_E	Q_o	$\frac{1}{2}\varepsilon_B$	Q_E	Q_o
Model A	.254	9.34	3360	420	1.35%	3820	445
Model B	.254	9.92	2700	510	< 1 %	3000	500
" "	.810	9.93	368	550	< 1 %	312	500

TABLE II

	Transformer Length	Observed Data λ_o	Q_E	Q_o
Model A	.25 λ_t	9.34	3360	420
" "	.278λ_t	9.35	3250	465
" "	.300λ_t	9.35	3400	420
Model B	.219λ_t	9.92	2700	510
" "	.244λ_t	9.91	2500	550
" "	.261λ_t	9.92	2600	550

An interesting although not very successful experiment with mode suppression was carried out in connection with the model tests. All cavity modes with n $\rangle$ 0 form degenerate pairs. For n = 2 the mode that can be excited from the wave guide has a mate with no coupling to the output system. A magnetron with such a resonator would tend to operate in the unloaded mode. The phase-reversing anode structure (Fig. 2B) may reduce this tendency but it does not eliminate it. Since modes of higher frequency than the desired one do not cause any trouble in a magnetron, the natural thing to do is to disturb the symmetry of the cavity in such a way that the resonance frequency of the undesired mode is moved to a higher frequency, while the desired one is substantially unaffected. In the test model this was done by short-circuiting the fingers placed at the nodes of the electric field in the desired mode (Fig. 2b) to the opposite wall of the cavity by means of small screws.

To the undesired mode these fingers then form high-susceptance inductive posts at the points of maximum electric field.

TABLE III

Test Cavity	Transformer Height	Observed Data with Mode Suppressors Applied λ_o	Q_E	Q_o
Model B	.254	9.85	1400	620
Model B	.810	9.85	185	585

However, the lower-order modes, n = 0 and n = 1, are affected in a similar way. In the test model the result was that the mode separation practically disappeared, the resonance wave lengths of the three lowest modes being 10.21, 10.02 and 9.84 cm for Model B (2t = .254 cm). The result of the impedance measurements are given above (Table III), subject to an important reservation: the procedure for computing Q from standing-wave measurements presupposes ample mode separation, consequently an appreciable error must be expected in this case. We shall, therefore, make no attempt to draw any conclusions from these data.

The result of this crude attempt at mode suppression is not discouraging. There are several obvious ways in which a further increase in the resonance frequency of the unwanted modes can be achieved.

In conclusion we can state that the results of the model tests are in satisfactory agreement with the calculations made according to the procedure proposed in this paper, although the measurements are neither extensive enough nor accurate enough to determine sharply the

limits of reliability of the method. The purpose of the tests was to give us confidence that the main principles of the method are sound and that we have not overlooked any of the important factors in the problem. Beyond that, we can judge the accuracy of the whole from the accuracy of the separate items. The most radical approximations concern the finger system, and since appreciable fractions of the total energy storage and copper losses are associated with the finger system, a certain error from this source is probable. Neglect or rough approximations of higher-order modes at the various junctions are other sources of errors, which can be estimated in each case. An interesting observation is that neglect of the proper transformation between the cylindrical waves in the cavity and the plane waves in the wave guide leads to an unexpectedly large error. For this reason it is the author's hope that particularly the formulas derived for this transformation will prove of value in design problems similar to the one treated above.

REFERENCES, PART I

1 Hahn, W.C., "A New Method for the Calculation of Cavity Resonators," Journal of Applied Physics, Vol. 12, pp. 62-68, January 1941

2 Slater, J.C., Microwave Transmission, McGraw-Hill, New York, 1942

3 Slater, J.C., Microwave Electronics, Van Nostrand, New York, 1949

4 Schelkunoff, S.A., Electromagnetic Waves, Van Nostrand, New York, 1943

5 Stratton, J.A., Electromagnetic Theory, McGraw-Hill, New York, 1941

6 Schwinger, J., "Discontinuities in Wave Guides," Notes from lectures at Radiation Laboratory, M.I.T., 1945

7 Whinnery, J.R., and Jameson, H.W., "Equivalent Circuits for Discontinuities in Transmission Lines," Proc. I.R.E., Vol. 32, pp. 98-February 1944

8 Miles, J.W., "The Equivalent Circuit for a Plane Discontinuity in a Cylindrical Wave Guide," Proc. I.R.E., Vol. 34, pp. 728-742, October 1946

9 Miles, J.W., "The Equivalent Circuit of a Corner Bend in a Rectangular Wave Guide," Proc. I.R.E., Vol. 35, pp. 1313-1317, November 1947

10 Marcuvitz, N., The Wave Guide Handbook, Vol. 10, Radiation Laboratory Series, McGraw-Hill, New York, 1951

REFERENCES, PART II

1 Crawford, F. H. and Hare, M. D., "Tunable Squirrel-Cage Magnetron - The Donutron," Proc. I. R. E., Vol. 35, pp. 361-369, April 1947

2 Lucke, W. S., "Obstacle-Loaded Cylindrical Cavities with Application to the Interdigital Magnetron," Technical Report No. 80, Cruft Laboratory, Harvard University, under Contract NR-ORl-76, Task Order No. 1, NR-078-011

3 Welch, H. W., Jr., and Brewer, G. R., "Operation of Interdigital Magnetrons in the Zero-Order Mode," Technical Report No. 2, Electron Tube Laboratory, Department of Electrical Engineering, University of Michigan

4 Hull, J. F. and Greenwalt, L. W., "Modes in Interdigital Magnetrons," Proc. I. R. E., Vol. 37, pp. 1258-1263, November 1949

5 Ramo, S. and Whinnery, J. R., Fields and Waves in Modern Radio, John Wiley and Sons, New York, 1944